

Aus dem Institut für Transfusionsmedizin  
der Medizinischen Fakultät Charité – Universitätsmedizin Berlin

DISSERTATION

**Thrombozyten-basierte und Thrombozyten nachahmende modifizierte  
Submikron-Partikel aus Humanserumalbumin zum Einfangen von Tu-  
morzellen**

**Platelet-based and platelet-mimicking modified human serum albu-  
min submicron particles for tumor cell capture**

zur Erlangung des akademischen Grades  
Doctor medicinae (Dr. med.)

vorgelegt der Medizinischen Fakultät  
Charité – Universitätsmedizin Berlin

von

Xiaotong Zhao

aus Jiangsu, China

Datum der Promotion: 30.11.2023



## Table of content

List of tables .....	iii
List of figures .....	iv
List of abbreviations.....	vi
Abstract .....	1
1 Introduction.....	4
1.1 Circulating tumor cells and hematogenous metastasis.....	4
1.2 Circulating tumor cells and platelets.....	4
1.3 Human serum albumin particles .....	5
1.4 The aim of this study .....	5
2 Methods.....	7
2.1 Platelets isolation.....	7
2.2 Cells .....	7
2.3 Activation of platelets under different shear rates.....	7
2.4 Adhesion of platelets to A549 cells.....	7
2.5 Protein expression of platelets adhesion receptors in lung adenocarcinoma ...	8
2.6 Preparation of HSA-MPs .....	8
2.7 Conjugation of anti-CD41 antibody or CD62P on the surface of HSA-MPs .....	8
2.8 The characterization of particles .....	9
2.9 The interaction between anti-CD41-HSA-MPs and platelets .....	9
2.10 The confirmation of the conjugation of CD62P with the HSA-MPs .....	9
2.11 Investigations from cellular uptake .....	9
2.12 The mRNA expression of CD62P ligands in TCGA and CCLE databases .....	10
2.13 Statistical analysis .....	10
3. Results .....	11
3.1 Characterization of anti-CD41-HSA-MPs and CD62P HSA-MPs .....	11
3.2 The platelets were activated under the high shear rates .....	11

---

3.3	A549 cells were adhered by platelets in <i>vitro</i> .....	12
3.4	Protein expression of platelets adhesion receptors in lung adenocarcinoma ...	13
3.5	Adhesion evaluation of anti-CD41-HSA-MPs to the platelets .....	15
3.6	Confirmation of the conjugation of CD62P with the HSA-MP .....	16
3.7	Increased cellular uptake of anti-CD41-HSA-MPs in A549 cells .....	17
3.8	Increased cellular uptake of CD62P-HSA-MPs in A549 cells .....	18
3.9	The mRNA expression of CD62P ligands in CCLE and TCGA databases.....	18
4.	Discussion .....	19
5.	Conclusions.....	23
	Reference list.....	24
	Statutory Declaration .....	29
	Declaration of your own contribution to the publications.....	30
	Excerpt from Journal Summary List.....	31
	Printing copy(s) of the publication(s) .....	35
	Curriculum Vitae .....	49
	Publication list.....	50
	Acknowledgments .....	51

## List of tables

**Table 1** (Page 21): The advantages and disadvantages of anti-CD41-HSA-MPs and CD62P-HSA-MPs drug delivery systems. (Own table)

## List of figures

**Figure 1** (Page 6): Schematic of targeting strategies. Anti-CD41-HSA-MPs track CTCs by hitchhiking on platelets; CD62P-HSA-MPs could mimic the adhesion function of platelets and target the CTCs directly via CD62P. (Modified from Xiaotong Zhao et al., 2022)

**Figure 2** (Page 11): The activation of platelets under different shearing rates. A. Representative histograms of the fluorescence intensity distribution in platelets under different shearing rates (0, 10, 100, 1000, 3000 s<sup>-1</sup>). B. The ratio of activated platelets under the different shear rates for 30 min. (Own figure)

**Figure 3** (Page 12): Adhesion between platelets and A549 cells in vitro. A. The dot plots showed the gating strategy. The A549 cells and platelets were distinguished by the FSC and SSC. The platelets were labeled with APC anti-CD41 antibody. The activated platelets were labeled with Alexa 647 anti-CD62P antibody. B. Histograms of the fluorescence intensity in the tumor cell population. C. Percentage of A549 cells with adhering platelets labeled with APC anti-CD41 antibody or Alexa 647 anti-CD62P antibody. D. Confocal laser scanning microscope analysis of platelets and A549 tumor cells at 3000 s<sup>-1</sup> shear rate. Platelets were stained with APC anti-CD41 antibody (red) and Alexa 488 anti-CD62P antibody (green). Yellow comes from the overlap of red and green fluorescence. (From Xiaotong Zhao et al., 2022)

**Figure 4** (Page 14): The IHC-based protein levels of platelets adhesion receptors in lung adenocarcinoma and normal lung tissues. Protein levels of CD44 in normal tissue (staining: not detected; intensity: negative; quantity: none); CD44 in tumor tissue (staining: medium; intensity: strong; quantity: <25%); SELPLG in normal tissue (staining: not detected; intensity: negative; quantity: none); SELPLG in tumor tissue (staining: not detected; intensity: negative; quantity: none); CD24 in normal tissue (staining: high; intensity: strong; quantity: 25–75%); CD24 in tumor tissue (staining: high; intensity: strong; quantity: 25–75%); Integrin  $\alpha$ V in normal tissue (staining: not detected; intensity: negative; quantity: none); Integrin  $\alpha$ V in tumor tissue (staining: high; intensity: strong; quantity: >75%); Integrin  $\beta$ 3 in normal tissue (staining: low; intensity: moderate; quantity: <25%); Integrin  $\beta$ 3 in tumor tissue (not detected; intensity: negative; quantity: none); PDPN in normal tissue (staining: medium; intensity: moderate; quantity: >75%); PDPN in tumor tissue (staining: low; intensity: weak; quantity: 25–

75%); HMGB1 in normal tissue (staining: high; intensity: strong; quantity: >75%); HMGB1 in tumor tissue (staining: high; intensity: strong; quantity: >75%). (Modified from the open-access database the Human Protein Atlas, 2023)

**Figure 5** (Page 16): The conjugation of CD62P with the HSA-MPs analyzed by flow cytometry. A. Dot plots of CD62P modified HSA-MPs, and CD62P modified HSA-MPs + Alexa 647 anti-CD62P antibody. The CD62P modified HSA-MPs were gated based on FSC and SSC. B. The typical histograms of the fluorescence intensity in the CD62P modified HSA-MPs population for HSA-MPs + Alexa 647 anti-CD62P antibody (control) and CD62P modified HSA-MPs + Alexa 647 anti-CD62P antibody. (Own figure)

**Figure 6** (Page 17): Adhesion vs. cellular uptake of anti-CD41-HSA-MPs and HSA-MP in A549 cells analyzed by flow cytometry with or without pre-incubation with activated platelets. Adhering particles are excluded by quenching with Trypan blue. Upper graphs show the percentage of events in the A549 cell population with enhanced fluorescence in the FITC channel. Lower graphs show the corresponding MFI.  $*P < 0.05$ . (From Xiaotong Zhao et al., 2022)

**Figure 7** (Page 18): Adhesion vs. cellular uptake of anti-CD62P-HSA-MPs and HSA-MP in A549 cells analyzed by flow cytometry. Adhering particles are excluded by quenching with Trypan blue. Upper graphs show the percentage of events in the A549 cell population with enhanced fluorescence in the FITC channel. Lower graphs show the corresponding MFI.  $*P < 0.05$ . (From Xiaotong Zhao et al., 2022)

## List of abbreviations

CTCs	Circulating Tumor Cells
CCD	Co-precipitation–Crosslinking–Dissolution
CCLE	Cancer Cell Lineage Encyclopedia
DMSO	Dimethyl Sulfoxide
EDC	1-Ethyl-3-(3-Dimethyl Aminopropyl) Carbodiimide Hydrochloride
EDTA	Ethylene Diamine Tetra-acetic Acid
EMT	Epithelial to Mesenchymal Transition
FITC	Fluorescein Isothiocyanate
FSC	Forward Scatter
GA	Glutaraldehyde
HPA	Human Protein Atlas
HSA	Human Serum Albumin
HSA-MPs	Human Serum Albumin-Submicron Particles
IHC	Immunohistochemistry
MES	2-(N-morpholino) Ethanesulfonic Acid
MFI	Mean Fluorescent Intensity
MnCl <sub>2</sub>	Magnesium Chloride
Na <sub>2</sub> CO <sub>3</sub>	Sodium Carbonate
NaBH <sub>4</sub>	Sodium Borohydride
NaOH	Sodium Hydroxide
NHS	N-hydroxysuccinimide
PBS	Phosphate-Buffered Saline
PDI	Poly Dispersity Index
PRP	Platelet-Rich Plasma
SSC	Sideward Scatter
Sulfo-NHS	N-Hydroxysulfosuccinimid
TCGA	The Cancer Genome Atlas
Tris	Tris (hydroxymethyl) aminomethane



## Abstract

**Objective:** It has long been understood that platelets and tumor cells colocalize in hematogenous metastases. Interactions between circulating tumor cells (CTCs) and platelets affect the survival and migration of tumor cells through the vascular system to other tissues. Here, based on the adhesion of activated platelets to CTCs, we designed two different modified submicron human serum albumin particles (HSA-MPs) to track the CTCs.

**Methods:** Co-precipitation–Cross-linking–Dissolution (CCD) technique was utilized to produce HSA-MPs. Separately, anti-CD41 antibody or CD62P protein was coupled to the HSA-MPs using EDC/NHS chemistry. Zetasizer was used to determine the characteristics of the prepared modified HSA-MPs. Platelet-rich plasma was subjected to a series of shear stress treatments, and CD62P expression was used to monitor the platelet activation. Fluorescence microscopy and flow cytometry were used to examine the interaction among platelets, anti-CD41-HSA-MPs, CD62P-HSA-MPs and the lung adenocarcinoma cell line A549 cells. We used bioinformatics techniques to gather and analyze datasets from the Cancer Cell Lineage Encyclopedia (CCLE) and The Cancer Genome Atlas (TCGA) databases to look for the expression of CD62P ligands, including CD44, SELPLG, and CD24, in diverse cancer types.

**Results:** HSA-MP showed a submicron size (0.9 to 1  $\mu\text{m}$ ) after conjugation with the anti-CD41 antibody or CD62P, and zeta potential was negative. In the absence of exogenous biochemical agonists, platelet exposure to continuous shear stress results in platelet activation. Under shearing conditions, we verified the adherence of platelets to A549 cells in vitro. In the presence of activated platelets, the cellular uptake of anti-CD41-HSA-MPs in A549 cells was observed to be higher compared to the plain HSA-MPs. The modification of CD62P on HSA-MPs increased the cellular uptake of HSA-MPs in A549. RNA-seq data from the CCLE and TCGA databases revealed that the major CD62P ligands were expressed in all tumor types and were significantly upregulated in 17 of 33 cancer types.

**Conclusion:** Our findings indicate that the platelet-based and platelet-mimicking modified HSA-MPs offer potential alternatives for detecting metastatic cancer.

## Zusammenfassung

**Zielsetzung:** Es ist seit langem bekannt, dass Thrombozyten und Tumorzellen in hämatogenen Metastasen kolokalisieren. Wechselwirkungen zwischen zirkulierenden Tumorzellen (CTCs) und Blutplättchen beeinflussen das Überleben und die Wanderung von Tumorzellen durch das Gefäßsystem in andere Gewebe. Indem wir die Wechselwirkungen zwischen Thrombozyten und Tumorzellen nutzen, haben wir zwei Strategien (eine direkte und eine indirekte) entwickelt, um modifizierte submikroskopische Humanserumalbuminpartikel (HSA-MPs) gezielt auf Tumorzellen zu richten.

**Methoden:** Zur Herstellung von HSA-MPs wurde die CCD-Technik (Co-Präzipitation-Cross-Linking-Dissolution) angewandt. Der Anti-CD41-Antikörper und das CD62P-Protein wurden separat mit Hilfe der EDC/NHS-Chemie an die HSA-MPs gekoppelt. Mit dem Zetasizer wurden die Eigenschaften der hergestellten modifizierten HSA-MPs bestimmt. Blutplättchenreiches Plasma wurde einer Reihe von Scherspannungsbehandlungen unterzogen, und die CD62P-Expression wurde verwendet, um die Aktivierung von Blutplättchen zu überwachen. Fluoreszenzmikroskopie und Durchflusszytometrie wurden verwendet, um die Wechselwirkung zwischen Blutplättchen, Anti-CD41-HSA-MPs, CD62P-HSA-MPs und den Zellen der Lungen-Adenokarzinom-Zelllinie A549-Zellen zu untersuchen. Mit bioinformatischen Techniken sammelten und analysierten wir Datensätze aus den Datenbanken Cancer Cell Lineage Encyclopedia (CCLE) und The Cancer Genome Atlas (TCGA), um die Expression von CD62P-Liganden, darunter CD44, SELPLG und CD24, in verschiedenen Krebsarten zu untersuchen.

**Ergebnisse:** HSA-MP wiesen nach Konjugation mit Anti-CD41-Antikörpern oder CD62P eine submikrone Größe (0,9 bis 1  $\mu\text{m}$ ) auf, und das Zeta-Potenzial war negativ. In Abwesenheit von exogenen biochemischen Agonisten führt die Exposition der Thrombozyten gegenüber einer kontinuierlichen Scherbelastung zu einer Aktivierung der Thrombozyten. Unter Scherungsbedingungen wurde die Adhärenz von Thrombozyten an A549-Zellen *in vitro* überprüft. In Gegenwart aktiver Thrombozyten wurde eine höhere zelluläre Aufnahme von Anti-CD41-HSA-MPs durch A549-Zellen beobachtet. CD62P-HSA-MPs zeigten im Vergleich zu nicht modifizierten HSA-MPs eine höhere Aufnahme durch A549-Zellen haben. RNA-seq-Daten aus den CCLE- und TCGA-Datenbanken zeigten, dass

die wichtigsten CD62P-Liganden in allen Tumorarten exprimiert wurden und in 17 von 33 Krebsarten signifikant hochreguliert waren.

Schlussfolgerung: Unsere Ergebnisse deuten darauf hin, dass die auf Thrombozyten basierenden und Thrombozyten nachahmenden modifizierten HSA-MPs potenzielle Alternativen für den Nachweis von metastasierendem Krebs darstellen.

# 1 Introduction

## 1.1 Circulating tumor cells and hematogenous metastasis

Hematogenous metastasis refers to the process of tumor cells running in circulation along with blood after invading blood vessels and attaching to the distal vascular endothelium. Hematogenous metastasis of tumor cells is significant in the whole process of tumor metastasis. In the process of tumor formation and growth, part of the tumor cells shed from the primary focus, enter the blood circulation system through the invasion of surrounding tissues and blood vessels to reach the distal tissues, and then proliferate and differentiate into secondary tumors in the new microenvironment, forming the distal metastasis [1]. These cells that enter the blood circulation system from the primary tumor are called circulating tumor cells (CTCs), which are the critical link of tumor metastasis. During the process of tumor metastasis, some CTCs will undergo epithelial-mesenchymal transformation (EMT) [2]. EMT, the process of tumor cells losing their epithelial characteristics and gaining mesenchymal characteristics, is believed to be the main cause of cancer cell spread. Survivor CTCs either squeeze through endothelial cells or co-opt the endothelium to leave the vasculature [3].

## 1.2 Circulating tumor cells and platelets

Platelets play a vital role in elevating the CTCs survival in the blood and promoting metastasis. Only a small percentage of CTCs enter the metastases due to harsh environmental conditions, such as shear stress, anoikis, and the immune system [4]. By recruiting and activating platelets, CTCs can survive in blood by having the activated platelets as a protective cloak [5, 6]. The platelet cloak could protect CTCs from shear stress or being cleared by immune cells, especially NK cells [7, 8]. Platelets-derived TGF $\beta$  and direct contacts between platelets and tumor cells can stimulate EMT in CTCs, which promotes cell invasion and metastasis [9]. Platelets are involved in tumor cell stasis in vessel walls by CD62P (P-selectin) and its ligand. The ATPs derived by platelets activated

the endothelial P2Y2 receptor, inducing vascular permeability and promoting the extravasation of tumor cells [10].

### 1.3 Human serum albumin particles

Human serum albumin (HSA) drug delivery vehicles have received much attention because of their capacity to interact with a variety of molecules as well as their nontoxicity, non-immunogenicity, and biocompatibility [11]. Several anticancer drugs, such as paclitaxel and methotrexate, have been shown to be effective when combined with albumin [12, 13]. Abraxane® (nanoparticle albumin-bound paclitaxel) is a therapeutic application of HSA medication delivery in cancer treatment [14, 15]. Our group has successfully developed the Co-precipitation–Crosslinking–Dissolution (CCD) technique to prepare Human serum albumin submicron particles (HSA-MPs) [16-18]. HSA-MPs manufactured using this method have been loaded with compounds and drugs in previous studies [19-21]. Although the HSA drug delivery system has broad application prospects and many advantages, improving the targeting ability needs to be considered and further studied.

### 1.4 The aim of this study

Inspired by the adhesion of platelet to the CTCs, we designed and discussed two HSA-based drug delivery systems: platelet-based particles (anti-CD41-HSA-MPs) and platelet-mimicking particles (CD62P-HSA-MPs).

- CD41, a heterodimer with a heavy chain and a light chain, is a reliable identification marker for platelets. Here, we coupled the anti-CD41 antibody to the HSA-MPs. It is hypothesized that anti-CD41 antibody-modified HSA-MP (anti-CD41-HSA-MP) will track tumor cells via hitching on platelets. The aggregation of platelets around tumor cells promotes the possibility of internalization of HSA-MPs through the albumin-binding proteins receptor, such as Gp60, SPARC, Gp18 and Gp30, on the surface of tumor cells.
- CD62P, a platelet activation marker, was translocated to the surface as platelets were activated. CD62P mediates the binding of platelets to endothelial cells, leukocytes, and cancer cells [22, 23]. The platelet-mimicking particles with CD62P (CD62P-HSA-

MPs) were constructed. The CD62P would enable the particles to recognize and target the receptors on tumor cells, such as CD44, SELPLG and CD24.

An overview of the strategies applied is seen in **Figure 1**.

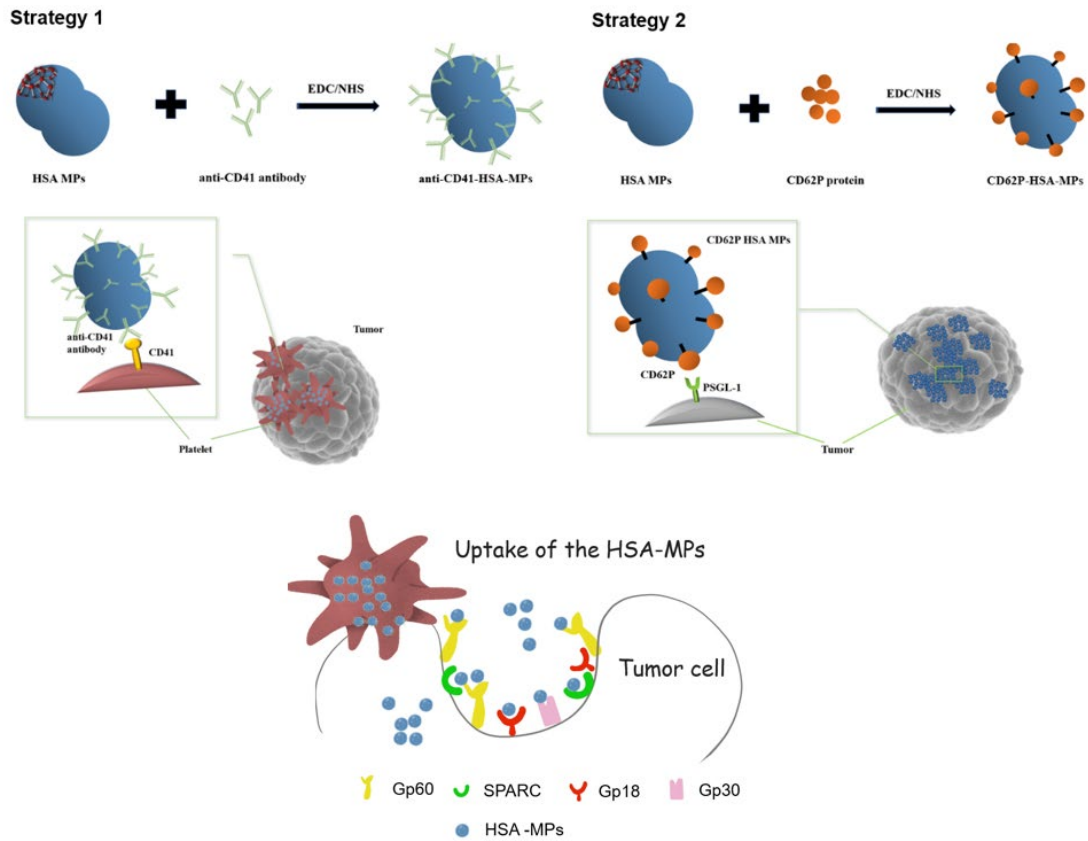


**Figure 1:** Schematic of targeting strategies. Anti-CD41-HSA-MPs track CTCs by hitchhiking on platelets; CD62P-HSA-MPs could mimic the adhesion function of platelets and target the CTCs directly via CD62P. (Modified from Xiaotong Zhao et al., 2022)

## 2 Methods

### 2.1 Platelets isolation

Blood was collected from healthy donors (EA1/110/21-Ethics committee Charité) in 0.105 M Na<sub>3</sub> citrate tubes (366575, BD Vacutainer). The whole blood was centrifugated at 150 g for 15 min to isolate the platelet-rich plasma (PRP).

### 2.2 Cells

Human lung adenocarcinoma cell line A549 was a kind gift of Prof. Sergio Moya (CIC bioma GUNE, San Sebastian, Spain). A549 cells were maintained in RPMI 1640 cell culture medium (Corning, New York, USA) supplemented with 10% fetal bovine serum (Bi-ochrom, Berlin, Germany) and 1% Penicillin-Streptomycin at 37°C and 5% CO<sub>2</sub> atmosphere.

### 2.3 Activation of platelets under different shear rates

In normal physiological conditions, platelet activation happens in response to several agonists as well as to high shear stress [24, 25]. In our study, a Rheometer was used to provide the shearing environment. PRP was obtained following the described above. 1ml PRP was placed in a high-performance Rheometer (Physica MCR 301, Anton Paar, Graz, Austria) under different shear rates (10, 100, 1000, 3000 s<sup>-1</sup>) at 37°C for 30 min. Then the PRP was incubated with Alexa 647 anti-CD62P antibody (BioLegend, San Diego, CA, USA) in the dark at 37°C for 20min. The activated platelets were labeled by CD62P antibody. Flow cytometry was used to explore the ratio of activated platelets.

### 2.4 Adhesion of platelets to A549 cells

The mixture of A549 cells and PRP at a tumor-platelet ratio of 1:250 were treated at 3000 s<sup>-1</sup> shear rate by a high-performance Rheometer at 37°C for 30 minutes. The samples were then incubated with specific antibodies (BioLegend, San Diego, CA, USA) for 20min to label the platelets. The flow cytometry (BD FACS Canto II, Franklin Lakes, NJ, USA) and confocal laser scanning microscope (CLSM ZeissLSM 510 meta, Zeiss MicroImaging GmbH, Jena, Germany) were used to explore the interaction between the A549 cells and platelets.

## 2.5 Protein expression of platelets adhesion receptors in lung adenocarcinoma

The Human Protein Atlas (HPA, <https://www.proteinatlas.org/>) is an open-access database that provides immunohistochemistry (IHC) staining images of cancer tissues and normal tissues [26]. To explore the possible mechanisms of the binding of platelets to the lung adenocarcinoma cells, we obtained and merged the protein expression IHC images of reported platelets adhesion receptors, including CD62P ligands (CD44, SELPLG, CD24), Podoplanin (PDPN) and HMGB1 in lung adenocarcinoma tissues from HPA.

## 2.6 Preparation of HSA-MPs

The HSA-MPs were prepared by the CCD method as described previously [16, 19, 20, 27]. In brief, 0.125 M manganese chloride ( $\text{MnCl}_2$ , Sigma-Aldrich, Munich, Germany) containing 10 mg/mL HSA (Grifols, Frankfurt, Germany) and 0.125 M sodium carbonate ( $\text{Na}_2\text{CO}_3$ , Sigma-Aldrich, Munich, Germany) were rapidly added in sequence under stirring for 30 s. 0.025 mg/ml fluorescein isothiocyanate (FITC, Sigma-Aldrich, Munich, Germany) in Dimethyl sulfoxide (DMSO, Carl Roth, Karlsruhe, Germany) was added as needed in the first step. The mixture was then mixed with 0.05% HSA solution and incubated for 5 minutes with stirring to prevent particle agglomeration. After being washed with 0.9% NaCl three times by centrifugation at 3000 g for 5 min, the particles were cross-linked by incubating with 0.1% glutaraldehyde (GA, Sigma-Aldrich, Munich, Germany) for 1 hour. Unbound GA was quenched by incubating with 0.08 M glycine (Sigma-Aldrich, Munich, Germany) and 0.625 mg/mL sodium borohydride ( $\text{NaBH}_4$ , Sigma-Aldrich, Munich, Germany) for 30min.  $\text{MnCO}_3$  templates were dissolved by incubation with 0.25 M Ethylene diamine tetra-acetic acid (EDTA, Fluka, Buchs, Switzerland) for another 30 min. The prepared particles were washed three times by centrifugation at 1000 g for 10 min and suspended in 0.9% NaCl solution.

## 2.7 Conjugation of anti-CD41 antibody or CD62P on the surface of HSA-MPs

The amino groups of anti-CD41 antibody were conjugated to the carboxyl groups of HSA-MPs via 1-ethyl-3-(3-dimethyl aminopropyl) carbodiimide hydrochloride (EDC) and N-hydroxysuccinimide (NHS) chemistry (EDC/NHS). HSA-MPs were washed and distributed in 50 mM MES buffer with a pH level of 6 (Thermo Scientific, Rockford, IL, USA). The washed 0.1% HSA-MP solution was incubated with 4.8 mM EDC (Thermo



Scientific, Rockford, IL, USA) and 48 mM NHS (Fluka, St. Louis, MO, USA) for 30 min at room temperature. To this, the anti-CD41 antibody (final concentration 10 µg/mL, Antibodies.com, Cambridge, UK) was added and mixed well for 2.5 hours. Glycine (final concentration 4 mg/mL) was added to quench the remaining NHS esters. Anti-CD41-HSA-MPs were washed three times and kept in the blocking buffer (50 mM Tris pH 8 and 0.5% HSA). CD62P-HSA-MPs were prepared by CD62P protein (Sino Biological, Eschborn, Germany) in the same way above (Figure 7 in [27]).

## **2.8 The characterization of particles**

The size and zeta potential of the modified HSA-MPs were determined by Zetasizer Nano ZS (Malvern Instruments Ltd., Malvern, UK). The particles were suspended in 10 mM NaCl and collected in a disposable cuvette for measuring particle size and a zeta cell for measuring zeta potential.

## **2.9 The interaction between anti-CD41-HSA-MPs and the platelets**

Anti-CD41-FITC-HSA-MPs were incubated in PRP at a particle-platelet ratio of 20:1 on the rotator for 30 min at 37°C. All the samples were fixed with 4% paraformaldehyde. Flow cytometry was used to analyze the fluorescence of particles on platelets in the FITC channel. The confocal laser scanning microscope also checked the interaction between anti-CD41-HSA-MPs and the platelets.

## **2.10 The confirmation of the conjugation of CD62P with the HSA-MPs**

The successful conjugation of CD62P with the HSA-MPs was confirmed by flow cytometry. The prepared CD62P modified HSA-MPs were incubated with Alexa 647 anti-CD62P antibody in the dark at 37°C for 20min. The CD62P-HSA-MPs were marked by CD62P antibody.

## **2.11 Investigations from cellular uptake**

A549 cells were seeded in a 24-well plate and grew for 24 hours. Before the treatment, the cells were washed with PBS. The activated platelets were gained by treating the PRP

with 5 µg/mL Arachidonic acid (Mölab, Langenfeld, German). The A549 cells were incubated with activated platelets at the platelets-tumor ratio of 250:1 for 30 min as needed. Then, the A549 cells with or without platelets were co-incubated with FITC-HSA-MPs, anti-CD41-FITC-HSA-MPs and CD62P-FITC-HSA-MPs in RPMI 1640 medium at a particle-tumor ratio of 5000:1 for 24 hours. Trypan blue was used to quench the remaining fluorescence on the surface of tumor cells as needed. All the samples were washed with PBS and fixed with 4% paraformaldehyde. The percentage of A549 cells with particles and MFI of A549 cells was calculated by the flow cytometer.

### **2.12 The mRNA expression of CD62P ligands in TCGA and CCLE databases**

CD44, SELPLG and CD24 are common ligands to CD62P. The Cancer Cell Line Encyclopedia (CCLE) project (<https://www.broadinstitute.org/ccle>) was used to explore the mRNA expression profiles of CD44 SELPLG and CD24 in 1091 types of cell lines. The Cancer Genome Atlas (TCGA) database (<https://portal.gdc.cancer.gov/>) was used to compare the mRNA expression of CD44, SELPLG and CD24 in 33 types of cancer tissues and corresponding para-cancer tissues. The data were analyzed by the Limma package in R software 4.10.

### **2.13 Statistical analysis**

Except for the statistical methods mentioned above, the difference between the groups was analyzed by the Student's *t*-test. Data were presented as mean ± standard deviations (*SD*). \**P* < 0.05, \*\**P* < 0.01, and \*\*\**P* < 0.001 were considered statistically significant.

### 3. Results

#### 3.1 Characterization of anti-CD41-HSA-MPs and CD62P-HSA-MPs

As was shown in Table 1 in [27], both anti-CD41-HSA-MPs and CD62P HSA-MPs had submicron sizes ( $952 \pm 41\text{nm}$  and  $974 \pm 15\text{nm}$ , respectively) and negative zeta potentials ( $-25 \pm 1$  and  $-24 \pm 2$ , respectively). Compared with HSA-MPs, anti-CD41-HSA-MPs and CD62P HSA-MPs sizes increased slightly. There are no significant differences in the zeta potential among the three types of particles.

#### 3.2 The platelets were activated under the high shear rates

In this experiment, a high-performance Rheometer was used to simulate the shear environment *in vivo*. CD62P, a transmembrane glycoprotein, is usually in platelet secretory  $\alpha$ -granules and Weibel-Palade bodies in endothelial cells. Once the platelets are activated, CD62P is rapidly mobilized to the surface of the platelets. CD62P was used as a platelet activation marker. The results indicated that the expression of CD62P increased along with the shearing rate. However, the increase in the expression of CD62P was not obvious from 10 to 1000  $\text{s}^{-1}$  shearing rates. The ratio of CD62P positive platelets was  $21.90 \pm 1.39\%$  at 3000  $\text{s}^{-1}$ , which was significantly higher than that of  $8.10 \pm 1.04\%$  at 10  $\text{s}^{-1}$ ,  $10.13 \pm 0.99\%$  at 100  $\text{s}^{-1}$  and  $15.30 \pm 2.51\%$  at 1000  $\text{s}^{-1}$  (**Figure 2**).

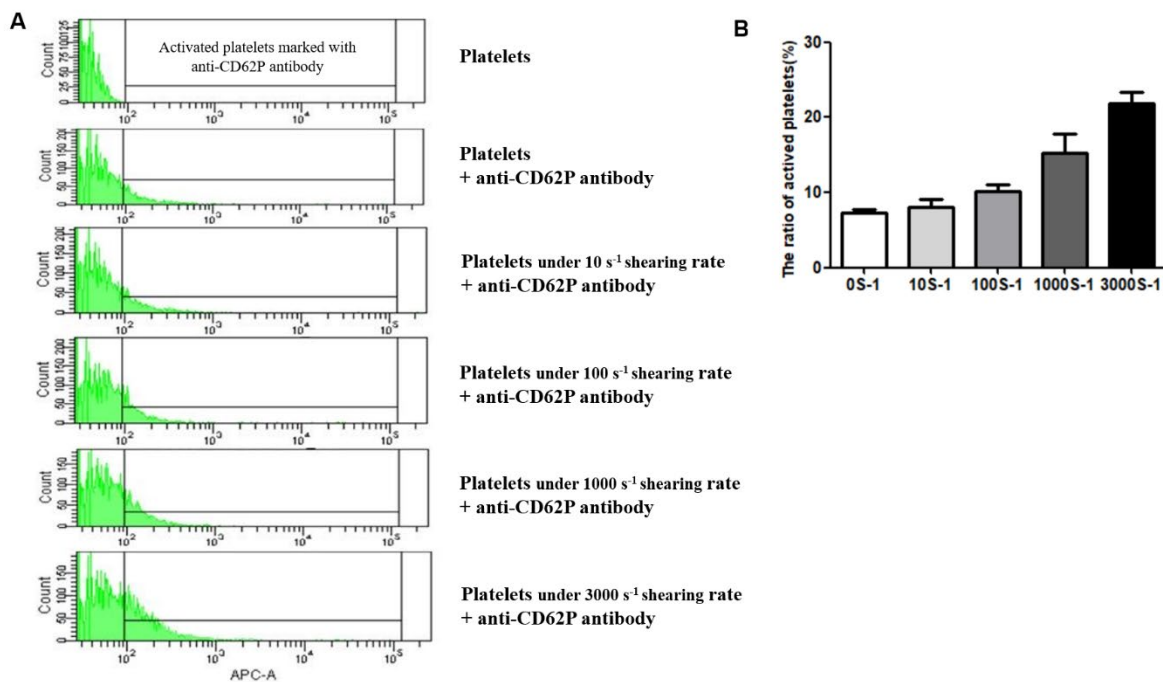


**Figure 2.** The activation of platelets under different shearing rates. A. Representative histograms of the fluorescence intensity distribution in platelets under different shearing rates (0, 10, 100, 1000, 3000  $s^{-1}$ ). B. The ratio of activated platelets under the different shear rates for 30 min. (Own figure)

### 3.3. A549 cells were adhered by platelets *in vitro*

Activated platelet adhesion to CTCs provided a crucial theoretical foundation for our research. Platelets collected from healthy donors and the A549 cells were placed at 3000  $s^{-1}$  shear rate to explore their interaction. Both the flow cytometer results and fluorescent images verified the adhesion between the activated platelets and the A549 cells (**Figure 3**). Anti-CD41 antibody was used to mark the platelets (including activated ones). Anti-CD62P antibody was used to mark the activated platelets. At the same time, we found that the anti-CD41 antibody labeled more platelets than the anti-CD62P antibody. This is probably because there are fewer activated platelets, and CD62 is a binding site for A549, so it cannot be simultaneously marked by fluorescent antibodies.

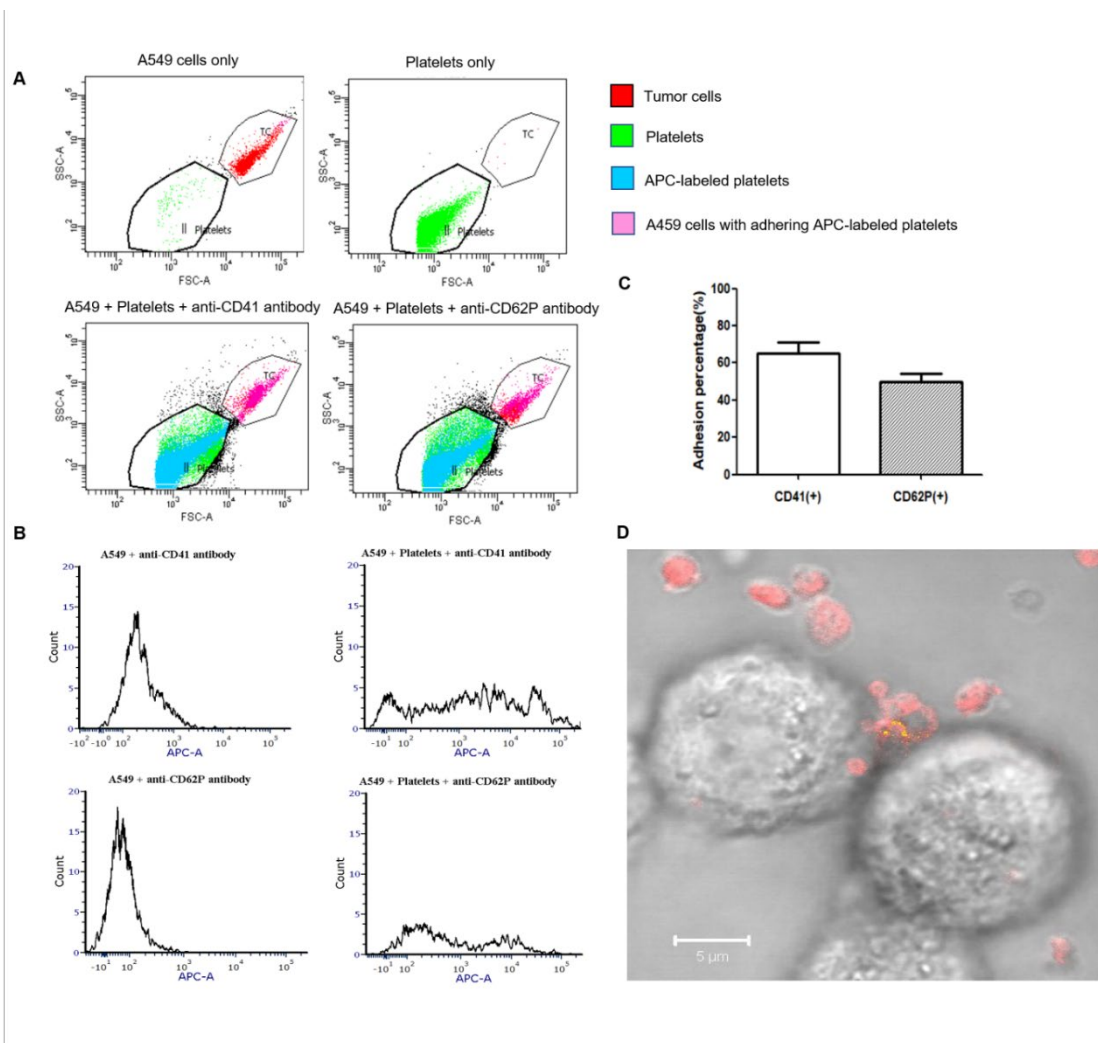


**Figure 3:** Adhesion between platelets and A549 cells *in vitro*. A. The dot plots showed the gating strategy. The A549 cells and platelets were distinguished by the FSC and SSC. The platelets were labeled with APC anti-CD41 antibody. The activated platelets were labeled with Alexa 647 anti-CD62P antibody. B. Histograms of the fluorescence intensity in the tumor cell population. C. Percentage of A549 cells with adhering platelets labeled with APC anti-CD41 antibody or Alexa 647 anti-CD62P antibody. D. Confocal laser scanning microscope analysis of platelets and A549 tumor cells at 3000 s<sup>-1</sup> shear rate. Platelets were stained with APC anti-CD41 antibody (red) and Alexa 488 anti-CD62P antibody (green). Yellow comes from the overlap of red and green fluorescence. (From Xiaotong Zhao et al., 2022)

### 3.4 Protein expression of platelets adhesion receptors in lung adenocarcinoma

As shown in **Figure 4**, The IHC results from the HPA database showed that all reported platelets adhesion receptors except SELPLG were expressed in lung adenocarcinoma tissues. The protein expression of CD44 and integrin  $\alpha V$  was higher in lung adenocarcinoma tissues than in normal lung tissues, while the protein expression of integrin  $\beta 3$  and PDPN were lower in lung adenocarcinoma tissues than in normal lung tissues. CD24 and HMGB1 proteins are highly expressed in normal and lung adenocarcinoma tissues. In addition, HMGB1 was only located in the nucleus, and other proteins were located in the Cytoplasm and the cell membrane. Given the protein expression levels and protein location on the membrane, CD44 and CD24 may involve in the platelet adhesion to the lung adenocarcinoma cells.

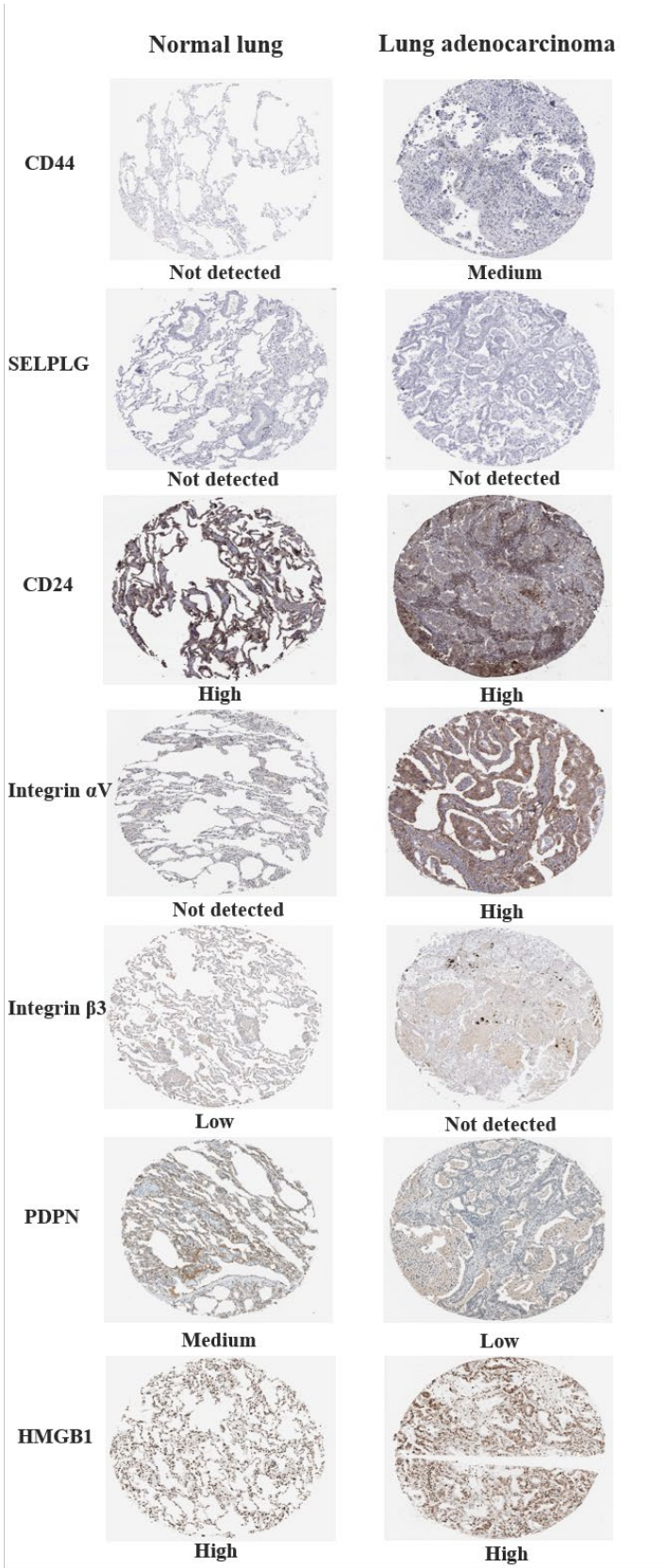


**Figure 4:** The IHC-based protein levels of platelets adhesion receptors in lung adenocarcinoma and normal lung tissues. Protein levels of CD44 in normal tissue (staining: not detected; intensity: negative; quantity: none); CD44 in tumor tissue (staining: medium; intensity: strong; quantity: <25%); SELPLG in normal tissue (staining: not detected; intensity: negative; quantity: none); SELPLG in tumor tissue (staining: not detected; intensity: negative; quantity: none); CD24 in normal tissue (staining: high; intensity: strong; quantity: 25–75%); CD24 in tumor tissue (staining: high; intensity: strong; quantity: 25–75%); Integrin  $\alpha$ V in normal tissue (staining: not detected; intensity: negative; quantity: none); Integrin  $\alpha$ V in tumor tissue (staining: high; intensity: strong; quantity: >75%); Integrin  $\beta$ 3 in normal tissue (staining: low; intensity: moderate; quantity: <25%); Integrin  $\beta$ 3 in tumor tissue (not detected; intensity: negative; quantity: none); PDPN in normal tissue (staining: medium; intensity: moderate; quantity: >75%); PDPN in tumor tissue (staining: low; intensity: weak; quantity: 25–75%); HMGB1 in normal tissue (staining: high; intensity: strong; quantity: >75%); HMGB1 in tumor tissue (staining: high; intensity: strong; quantity: >75%). (Modified from the open-access database the Human Protein Atlas, 2023)

### 3.5 Adhesion evaluation of anti-CD41-HSA-MPs to the platelets

In order to verify the successful preparation and effectiveness of anti-CD41-HSA-MPs, we evaluated the ability of anti-CD41-HSA-MPs to adhere to the platelets *in vitro*. The flow cytometry and confocal laser scanning microscope results suggested that there was more adhesion of anti-CD41-HSA-MPs than HSA-MPs to the A549 cells *in vitro* (Figure 3 in [27]). A similar percentage of platelets with particles was observed between the anti-CD41-HSA-MPs group and the HSA-MPs group (control). However, the percentage of platelets with adhered MPs did not reflect the exact number of adhered particles. And then, we measured the MFI of platelets, which reflected the adhesion of particles to a single platelet. The MFI in the anti-CD41-HSA-MPs group was nearly twice that in the HSA-MPs group. The difference was statistically significant. In general, there may be some nonspecific adhesion of HSA-MPs to the platelets, but there is still a difference in adhesion ability between anti-CD41-HSA-MPs and HSA-MPs.



### 3.6 Confirmation of the conjugation of CD62P with the HSA-MPs

Unlike anti-CD41 antibodies, the successful conjugation of CD62P to the particles can be verified by the staining of anti-CD62P antibodies on the particles. As shown in **Figure 5**, after the conjugation of CD62P with the HSA-MPs by EDC/NHS method, most CD62P modified HSA-MPs were labeled with anti-CD62P antibody, which indicated that the HSA-MPs were coupled with CD62P successfully.

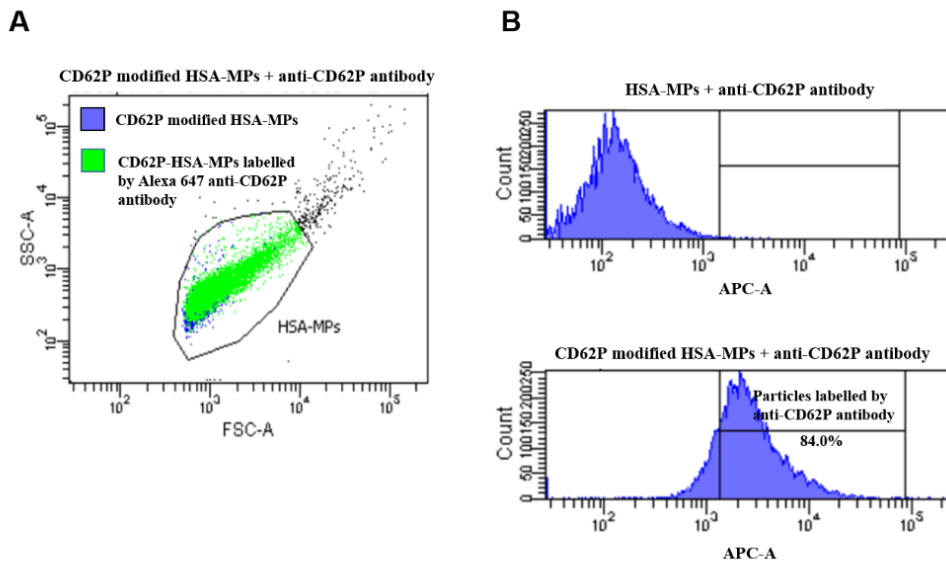


**Figure 5:** The conjugation of CD62P with the HSA-MPs analyzed by flow cytometry. A. Dot plots of CD62P modified HSA-MPs, and CD62P modified HSA-MPs + Alexa 647 anti-CD62P antibody. The CD62P modified HSA-MPs were gated based on FSC and SSC. B. The typical histograms of the fluorescence intensity in the CD62P modified HSA-MPs population for HSA-MPs + Alexa 647 anti-CD62P antibody (control) and CD62P modified HSA-MPs + Alexa 647 anti-CD62P antibody. (Own figure)



### 3.7 Increased cellular uptake of anti-CD41-HSA-MPs in A549 cells

To explore the cellular uptake of anti-CD41-HSA-MPs in A549 cells, we incubated A549 cells (pre-incubated with arachidonic acid-activated platelets for 30min) with FITC labeled anti-CD41-HSA-MPs for 24h. In the presence of platelets, a significantly higher cellular uptake of anti-CD41-HSA-MPs was found than HSA-MPs. In the absence of the platelets, there was no difference in cellular uptake between the anti-CD41-HSA-MPs and HSA-MPs. Meanwhile, similar results were gained when the Trypan blue was used to quench the extracellular fluorescence (**Figure 6**).

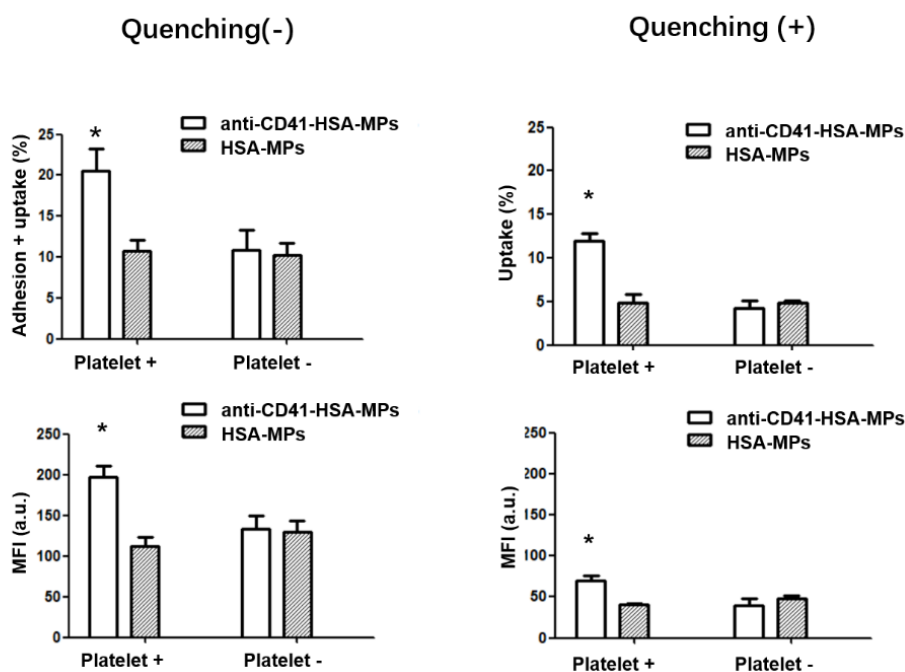


**Figure 6:** Adhesion vs. cellular uptake of anti-CD41-HSA-MPs and HSA-MP in A549 cells analyzed by flow cytometry, with or without pre-incubation with activated platelets. Adhering particles are excluded by quenching with Trypan blue. Upper graphs show the percentage of events in the A549 cell population with enhanced fluorescence in the FITC channel. Lower graphs show the corresponding MFI. \* $P < 0.05$ . (From Xiaotong Zhao et al., 2022)

### 3.8 Increased cellular uptake of CD62P-HSA-MPs in A549 cells

Before flow cytometry analysis, we incubated the CD62P-HSA-MPs or HSA-MPs with A549 cells for 24 hours. The results showed that the cellular uptake percentage and MFI in the CD62P-HSA-MPs group were both higher than those in the HSA-MPs group with or without quenching, which indicated that HSA-MPs could be internalized more efficiently when they were modified with CD62P (**Figure 7**).

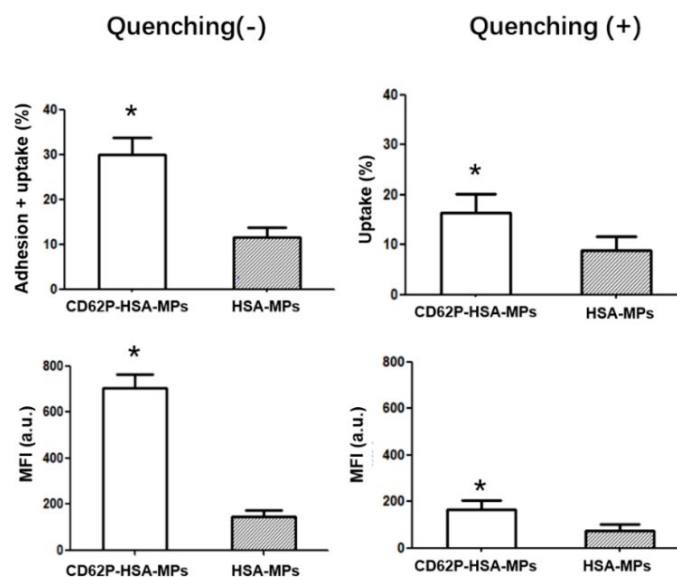


**Figure 7:** Adhesion vs. cellular uptake of anti-CD62P-HSA-MPs and HSA-MP in A549 cells analyzed by flow cytometry. Adhering particles are excluded by quenching with Trypan blue. Upper graphs show the percentage of events in the A549 cell population with enhanced fluorescence in the FITC channel. Lower graphs show the corresponding MFI. \* $P < 0.05$ . (From Xiaotong Zhao et al., 2022)

### 3.9 The mRNA expression of CD62P ligands in CCLE and TCGA databases

Using TCGA and CCLE datasets, we identified the expression of common ligands for CD62P (CD44, SELPLG, and CD24) in different types of tumor cell lines and tissues. According to RNA-seq data from the CCLE database, ligands for CD62P were expressed in nearly all types of tumors. Based on our analysis of the TCGA database, the expression of ligands was significantly higher in 17 cancers out of 33 types of cancers (Figure 6 in [27]). The preceding results supported the use of CD62P-HSA-MPs universally in tumor capture.

## 4. Discussion

The development of tumor is closely related to platelets. Tumor cells can activate platelets, causing them to accumulate in circulation. Platelets help maintain the integrity of the tumor vascular system and are involved in multiple steps of metastasis [28]. Elevated platelet counts are considered a marker of poor prognosis for many types of cancer [29-31]. Platelets activated by tumor cells promote tumor growth and metastasis and protect CTCs from the immune system and anoikis. Great potential has emerged to harness the function of platelets to design drug-delivery systems to treat tumors. Based on widely reported interactions between platelets and tumor cells, some researchers have developed CTC-targeted medicinal treatments utilizing platelet-mediated drug delivery systems, such as platelet engineering and membrane coating. For instance, platelets were decorated with anti-PD-L1 antibodies and anti-PD-1 antibodies to treat breast carcinomas and leukaemia [32, 33]; Electroporation is used to load gold nanorods in the platelets for photothermal therapy of head and neck cancer [34]. Li et al. genetically engineered hematopoietic stem cells and progenitor cells (HSPCS) to produce platelets expressing TRAIL proteins to track and kill tumor cells [35]. Platelet membrane coating on particles is another strategy that has been discussed [36, 37]. Although genetic engineering technology has advantages in efficient mass production, in vitro processing of platelets requires complex preparation and rigorous platelet examination. Platelet products are stored at the proper temperature to retain their integrity and function. Strict storage requirements of platelets result in a low supply, a short shelf life, and a high contamination potential. In addition, platelets play a negative role in thrombosis and tumor development and using platelets as drug carriers may lead to the risk of tumor-related thrombosis and the deterioration of tumor progression after re-transfusion [38]. Therefore, using autologous platelets to target tumors is a better option than using additional platelets modified in vitro. Moreover, using particles to simulate the function of platelets is also a great way to reduce the adverse effects brought by exogenous platelets.

Activated platelet adhesion to CTCs provided a crucial theoretical foundation for our research. The Rheometer was used to provide a shearing environment in our study. The activation markers on the platelets, such as CD62P, GPIIb/IIIa, and lysosomal glycoprotein, will be highly expressed significantly after transient exposure of the platelets to higher shear forces [25]. Our results were consistent with previous research. In our study,

we confirmed the activation of platelets at different shear rates by the measurement of platelet activation marker CD62P. Then we found the adhesion of platelets to the A549 cells at a high shear rate through flow cytometry and the microscope. The translocation of specific proteins, such as CD62P, to the surface of platelets under shear conditions may contribute to the adhesion between platelets and the tumor cells.

In this study, the lung adenocarcinoma cell line A549 was used as a representative to study the relationship between modified HSA-MPs and tumor cells. The primary albumin-binding proteins overexpressed in many cancers include Gp60, SPARC, Gp18, and Gp30. They mediate albumin absorption in the tumor by facilitating transcytosis across endothelium and endocytosis within tumor cells [39-41]. Because albumin can be endocytosed by alveolar epithelial cells via the Gp60 albumin receptor, the A549 cell is a good model for studying the cellular uptake of albumin particles [19, 42, 43]. In addition, since platelet adhesion receptors were found in lung adenocarcinoma tissues in the Human Protein Atlas database, the A549 cell line is also a good choice to study the interaction between platelets and tumor cells.

It is essential to mention that the number of activated platelets in the blood is relatively low. In normal physiological blood flow, the wall shear rate ranges from around  $10\text{ s}^{-1}$  in the vein to about  $2000\text{ s}^{-1}$  in the minimal arteries [44]. Most platelets in normal circulation are at rest. A large number of platelets are activated only under certain conditions, for example, pathological conditions or bleeding. CD41 is a platelet-expressed heterodimer consisting of a heavy chain and a light chain connected by a single disulfide bond. Considering the specific and stable expression of CD41 on platelets, CD41 is an ideal binding site between HSA-MPs and platelets. Given the difference in the number of activated and resting platelets, hitchhiking of anti-CD41-HSA-MPs on activated platelets under pathologic conditions is more efficient than hitchhiking on activated platelets only. After 24h coincubation with activated platelets pre-incubated A549 cells, the platelets-adhering anti-CD41-HSA-MPs were internalized more efficiently than the HSA-MPs by A549 cells. The results could be explained by platelets serving as a connection between anti-CD41-HSA-MPs and tumor cells. Hitchhiking of HSA-MP on platelets enhances the binding efficacy of HSA-MPs to the tumor cells. The results suggest that anti-CD41-HSA-MPs can be used to detect tumor cells utilizing circulating platelets and are also promising for the delivery of anticancer drugs without an ex vivo treatment of platelets.

Tumor cells could express different binding proteins that mediate the adhesion of platelets. CD62P on activated platelets could interact directly with SELPLG (PSGL-1) expressing on tumor cells [45, 46]. It was demonstrated that the glycoproteins with sialyl-Lewis structures on the tumor cell were involved in CD62P binding [46]. CD44 on tumor cells also mediates adhesion to CD62P-expressed platelets directly or indirectly [47].

In addition to CD62P-CD62P ligands, integrin  $\alpha$ IIb $\beta$ 3-fibrinogen- $\alpha$ V $\beta$ 3, CLEC-2–Podoplanin (PDPN), and TLR4-HMGB1 are involved in the platelet activation and adhesion of platelets to the tumor cells [48-50]. In the research of the platelet-tumor cell interactions and the specific molecular mechanisms, studies on CD62P and its ligands are extensive and comprehensive. Cancer patients were shown to have significantly higher levels of CD62P expression on platelets in their blood compared to healthy individuals [51]. Furthermore, other CD62P ligands (CD44, SELPLG, and CD24) have been found to be highly expressed in various human carcinomas [52-58]. In our study, a significantly higher cellular uptake of CD62P-HSA-MPs was found. When testing platelet-mimicking carriers targeting tumor cells in practical drug delivery applications, tumor cells should be compared to noncancerous cells with limited platelet binding capacity. In this instance, a higher level of targeted binding with tumor cells is more conducive to the use of a delivery system. By bioinformatics analysis, the main CD62P ligands, including CD44, SELPLG and CD24, were expressed in almost all types of tumor cells and were significantly higher in 17 out of 33 types of cancers, which provided a basis for the application of the CD62P-based albumin tumor-targeting carrier in tracking different types of CTCs.

Both anti-CD41-HSA-MPs and CD62P-HSA-MPs drug delivery systems have their own advantages and disadvantages. Here, we describe them briefly (**Table 1**).

**Table 1:** The advantages and disadvantages of anti-CD41-HSA-MPs and CD62P-HSA-MPs drug delivery systems. (Own table)

Particles	Advantages	Disadvantages
anti-CD41-HSA-MPs	<ul style="list-style-type: none"> <li>● No need for exogenous platelets</li> <li>● No need for the same strict storage requirements as platelets</li> <li>● High yield</li> </ul>	<ul style="list-style-type: none"> <li>● Dependence on the presence and the status of platelets</li> </ul>
CD62P-HSA-MPs		<ul style="list-style-type: none"> <li>● A single binding site to the tumors compared to the complete platelet</li> </ul>

We acknowledge that a physiological setting and a single-cell experimental environment are different, such as the presence of other blood cells and a complex hemodynamic environment. The interactions delivery system and tumor cells may vary depending on the environment. In previous investigations, we have demonstrated that HSA-MPs do not influence the function of platelets and do not interact with blood cells (no increase of activated platelets, no reduction of platelet activation after adding agonists, no significant change of the flow properties of whole blood, no significant increase of the phagocytosis rate) [20]. The results help us further in the next step to develop a targeted and sustained drug delivery system. Even so, further experimental in vivo and clinical tests are still necessary.

## 5. Conclusions

In summary, we developed two different modified HSA-MPs to track the CTCs. Anti-CD41-HSA-MPs were designed to target CTCs by hitchhiking on platelets. CD62P-HSA-MPs were designed to target CTCs directly by CD62P. In vitro, both particles can selectively recognize and be successfully taken up by A549 cells. These findings demonstrate that platelet-based and platelet-mimicking HSA-MPs have promising potential for selective targeting in cancer monitoring and therapy.

## Reference list

1. Kim MY, Oskarsson T, Acharyya S, Nguyen DX, Zhang XH, Norton L and Massague J (2009) Tumor self-seeding by circulating cancer cells. *Cell* 139:1315-26. doi: 10.1016/j.cell.2009.11.025
2. Dongre A and Weinberg RA (2019) New insights into the mechanisms of epithelial-mesenchymal transition and implications for cancer. *Nat Rev Mol Cell Biol* 20:69-84. doi: 10.1038/s41580-018-0080-4
3. Follain G, Osmani N, Azevedo AS, Allio G, Mercier L, Karreman MA, Solecki G, Garcia Leon MJ, Lefebvre O, Fekonja N, Hille C, Chabannes V, Dolle G, Metivet T, Hovsepian F, Prudhomme C, Pichot A, Paul N, Carapito R, Bahram S, Ruthensteiner B, Kemmling A, Siemonsen S, Schneider T, Fiehler J, Glatzel M, Winkler F, Schwab Y, Pantel K, Harlepp S and Goetz JG (2018) Hemodynamic Forces Tune the Arrest, Adhesion, and Extravasation of Circulating Tumor Cells. *Dev Cell* 45:33-52 e12. doi: 10.1016/j.devcel.2018.02.015
4. Peralta M, Osmani N and Goetz JG (2022) Circulating tumor cells: Towards mechanical phenotyping of metastasis. *iScience* 25:103969. doi: 10.1016/j.isci.2022.103969
5. Gay LJ and Felding-Habermann B (2011) Contribution of platelets to tumour metastasis. *Nat Rev Cancer* 11:123-34. doi: 10.1038/nrc3004
6. Li N (2016) Platelets in cancer metastasis: To help the "villain" to do evil. *Int J Cancer* 138:2078-87. doi: 10.1002/ijc.29847
7. Labelle M and Hynes RO (2012) The initial hours of metastasis: the importance of cooperative host-tumor cell interactions during hematogenous dissemination. *Cancer Discov* 2:1091-9. doi: 10.1158/2159-8290.CD-12-0329
8. Bambace NM and Holmes CE (2011) The platelet contribution to cancer progression. *J Thromb Haemost* 9:237-49. doi: 10.1111/j.1538-7836.2010.04131.x
9. Labelle M, Begum S and Hynes RO (2011) Direct signaling between platelets and cancer cells induces an epithelial-mesenchymal-like transition and promotes metastasis. *Cancer Cell* 20:576-90. doi: 10.1016/j.ccr.2011.09.009
10. Schumacher D, Strilic B, Sivaraj KK, Wettschureck N and Offermanns S (2013) Platelet-derived nucleotides promote tumor-cell transendothelial migration and metastasis via P2Y2 receptor. *Cancer Cell* 24:130-7. doi: 10.1016/j.ccr.2013.05.008
11. Karimi M, Bahrami S, Ravari SB, Zangabad PS, Mirshekari H, Bozorgomid M, Shahreza S, Sori M and Hamblin MR (2016) Albumin nanostructures as advanced drug delivery systems. *Expert Opin Drug Deliv* 13:1609-1623. doi: 10.1080/17425247.2016.1193149
12. Bolling C, Graefe T, Lubbing C, Jankevicius F, Uktveris S, Cesas A, Meyer-Moldenhauer WH, Starkmann H, Weigel M, Burk K and Hanauske AR (2006) Phase II study of MTX-HSA in combination with cisplatin as first line treatment in patients with advanced or metastatic transitional cell carcinoma. *Invest New Drugs* 24:521-7. doi: 10.1007/s10637-006-8221-6
13. Vis AN, van der Gaast A, van Rhijn BW, Catsburg TK, Schmidt C and Mickisch GH (2002) A phase II trial of methotrexate-human serum albumin (MTX-HSA) in patients with metastatic renal cell carcinoma who progressed under immunotherapy. *Cancer Chemother Pharmacol* 49:342-5. doi: 10.1007/s00280-001-0417-z
14. Fabi A, Giannarelli D, Malaguti P, Ferretti G, Vari S, Papaldo P, Nistico C, Caterino M, De Vita R, Mottolese M, Iacorossi L and Cognetti F (2015) Prospective study on nanoparticle albumin-bound paclitaxel in advanced breast cancer: clinical results and



- biological observations in taxane-pretreated patients. *Drug Des Devel Ther* 9:6177-83. doi: 10.2147/DDDT.S89575
15. Murphy C, Muscat A, Ashley D, Mukaro V, West L, Liao Y, Chisanga D, Shi W, Collins I, Baron-Hay S, Patil S, Lindeman G and Khasraw M (2019) Tailored NEOadjuvant epirubicin, cyclophosphamide and Nanoparticle Albumin-Bound paclitaxel for breast cancer: The phase II NEONAB trial-Clinical outcomes and molecular determinants of response. *PLoS One* 14:e0210891. doi: 10.1371/journal.pone.0210891
  16. Baumler H and Georgieva R (2010) Coupled enzyme reactions in multicompart ment microparticles. *Biomacromolecules* 11:1480-7. doi: 10.1021/bm1001125
  17. Xiong Y, Liu ZZ, Georgieva R, Smuda K, Steffen A, Sendeski M, Voigt A, Patzak A and Baumler H (2013) Nonvasoconstrictive hemoglobin particles as oxygen carriers. *ACS Nano* 7:7454-61. doi: 10.1021/nn402073n
  18. Xiong Y, Steffen A, Andreas K, Muller S, Sternberg N, Georgieva R and Baumler H (2012) Hemoglobin-based oxygen carrier microparticles: synthesis, properties, and in vitro and in vivo investigations. *Biomacromolecules* 13:3292-300. doi: 10.1021/bm301085x
  19. Chaiwaree S, Prapan A, Suwannasom N, Laporte T, Neumann T, Pruss A, Georgieva R and Baumler H (2020) Doxorubicin-Loaded Human Serum Albumin Submicron Particles: Preparation, Characterization and In Vitro Cellular Uptake. *Pharmaceutics* 12. doi: 10.3390/pharmaceutics12030224
  20. Suwannasom N, Smuda K, Kloypan C, Kaewprayoon W, Baisaeng N, Prapan A, Chaiwaree S, Georgieva R and Baumler H (2019) Albumin Submicron Particles with Entrapped Riboflavin-Fabrication and Characterization. *Nanomaterials (Basel)* 9. doi: 10.3390/nano9030482
  21. Jantakee K, Prapan A, Chaiwaree S, Suwannasom N, Kaewprayoon W, Georgieva R, Tragoolpua Y and Baumler H (2021) Fabrication and Characterization of Human Serum Albumin Particles Loaded with Non-Sericin Extract Obtained from Silk Cocoon as a Carrier System for Hydrophobic Substances. *Polymers (Basel)* 13. doi: 10.3390/polym13030334
  22. Kim YJ, Borsig L, Han HL, Varki NM and Varki A (1999) Distinct selectin ligands on colon carcinoma mucins can mediate pathological interactions among platelets, leukocytes, and endothelium. *Am J Pathol* 155:461-72. doi: 10.1016/S0002-9440(10)65142-5
  23. Chen M and Geng JG (2006) P-selectin mediates adhesion of leukocytes, platelets, and cancer cells in inflammation, thrombosis, and cancer growth and metastasis. *Arch Immunol Ther Exp (Warsz)* 54:75-84. doi: 10.1007/s00005-006-0010-6
  24. Holme PA, Orvim U, Hamers MJ, Solum NO, Brosstad FR, Barstad RM and Sakariassen KS (1997) Shear-induced platelet activation and platelet microparticle formation at blood flow conditions as in arteries with a severe stenosis. *Arterioscler Thromb Vasc Biol* 17:646-53. doi: 10.1161/01.atv.17.4.646
  25. Rahman SM and Hlady V (2019) Downstream platelet adhesion and activation under highly elevated upstream shear forces. *Acta Biomater* 91:135-143. doi: 10.1016/j.actbio.2019.04.028
  26. Ponten F, Jirstrom K and Uhlen M (2008) The Human Protein Atlas--a tool for pathology. *J Pathol* 216:387-93. doi: 10.1002/path.2440
  27. Zhao X, Georgieva R, Rerkshanandana P, Hackmann M, Heil Olaizola LE, Muller-de Ahna M and Baumler H (2022) Tumor Cell Capture Using Platelet-Based and Platelet-Mimicking Modified Human Serum Albumin Submicron Particles. *Int J Mol Sci* 23. doi: 10.3390/ijms232214277

28. Haemmerle M, Stone RL, Menter DG, Afshar-Kharghan V and Sood AK (2018) The Platelet Lifeline to Cancer: Challenges and Opportunities. *Cancer Cell* 33:965-983. doi: 10.1016/j.ccell.2018.03.002
29. Zhou Q, Huang F, He Z and Zuo MZ (2018) Clinicopathological and prognostic significance of platelet count in patients with ovarian cancer. *Climacteric* 21:60-68. doi: 10.1080/13697137.2017.1406911
30. Sasaki K, Kawai K, Tsuno NH, Sunami E and Kitayama J (2012) Impact of preoperative thrombocytosis on the survival of patients with primary colorectal cancer. *World J Surg* 36:192-200. doi: 10.1007/s00268-011-1329-7
31. Ishibashi Y, Tsujimoto H, Sugasawa H, Kouzu K, Itazaki Y, Sugihara T, Harada M, Ito N, Kishi Y and Ueno H (2021) Prognostic value of platelet-related measures for overall survival in esophageal squamous cell carcinoma: A systematic review and meta-analysis. *Crit Rev Oncol Hematol* 164:103427. doi: 10.1016/j.critrevonc.2021.103427
32. Han X, Chen J, Chu J, Liang C, Ma Q, Fan Q, Liu Z and Wang C (2019) Platelets as platforms for inhibition of tumor recurrence post-physical therapy by delivery of anti-PD-L1 checkpoint antibody. *J Control Release* 304:233-241. doi: 10.1016/j.jconrel.2019.05.008
33. Hu Q, Sun W, Wang J, Ruan H, Zhang X, Ye Y, Shen S, Wang C, Lu W, Cheng K, Dotti G, Zeidner JF, Wang J and Gu Z (2018) Conjugation of haematopoietic stem cells and platelets decorated with anti-PD-1 antibodies augments anti-leukaemia efficacy. *Nat Biomed Eng* 2:831-840. doi: 10.1038/s41551-018-0310-2
34. Rao L, Bu LL, Ma L, Wang W, Liu H, Wan D, Liu JF, Li A, Guo SS, Zhang L, Zhang WF, Zhao XZ, Sun ZJ and Liu W (2018) Platelet-Facilitated Photothermal Therapy of Head and Neck Squamous Cell Carcinoma. *Angew Chem Int Ed Engl* 57:986-991. doi: 10.1002/anie.201709457
35. Li J, Sharkey CC, Wun B, Liesveld JL and King MR (2016) Genetic engineering of platelets to neutralize circulating tumor cells. *J Control Release* 228:38-47. doi: 10.1016/j.jconrel.2016.02.036
36. Hu Q, Sun W, Qian C, Wang C, Bomba HN and Gu Z (2015) Anticancer Platelet-Mimicking Nanovehicles. *Adv Mater* 27:7043-50. doi: 10.1002/adma.201503323
37. Li J, Ai Y, Wang L, Bu P, Sharkey CC, Wu Q, Wun B, Roy S, Shen X and King MR (2016) Targeted drug delivery to circulating tumor cells via platelet membrane-functionalized particles. *Biomaterials* 76:52-65. doi: 10.1016/j.biomaterials.2015.10.046
38. Ay C, Simanek R, Vormittag R, Dunkler D, Alguel G, Koder S, Kornek G, Marosi C, Wagner O, Zielinski C and Pabinger I (2008) High plasma levels of soluble P-selectin are predictive of venous thromboembolism in cancer patients: results from the Vienna Cancer and Thrombosis Study (CATS). *Blood* 112:2703-8. doi: 10.1182/blood-2008-02-142422
39. Desai N, Trieu V, Damascelli B and Soon-Shiong P (2009) SPARC Expression Correlates with Tumor Response to Albumin-Bound Paclitaxel in Head and Neck Cancer Patients. *Transl Oncol* 2:59-64. doi: 10.1593/tlo.09109
40. Merlot AM, Kalinowski DS and Richardson DR (2014) Unraveling the mysteries of serum albumin-more than just a serum protein. *Front Physiol* 5:299. doi: 10.3389/fphys.2014.00299
41. Schnitzer JE and Oh P (1994) Albondin-mediated capillary permeability to albumin. Differential role of receptors in endothelial transcytosis and endocytosis of native and modified albumins. *J Biol Chem* 269:6072-82.
42. Chen J-L, Peng S-W, Ko W-H, Yeh M-K and Chiang C-H (2015) The mechanism of high transfection efficiency of human serum albumin conjugated polyethylenimine in A549 cells. *Journal of Medical Sciences* 35. doi: 10.4103/1011-4564.156009

43. Yumoto R, Suzuka S, Oda K, Nagai J and Takano M (2012) Endocytic uptake of FITC-albumin by human alveolar epithelial cell line A549. *Drug Metab Pharmacokinet* 27:336-43. doi: 10.2133/dmpk.dmpk-11-rg-127
44. Sakariassen KS, Orning L and Turitto VT (2015) The impact of blood shear rate on arterial thrombus formation. *Future Sci OA* 1:FSO30. doi: 10.4155/fso.15.28
45. Kim YJ, Borsig L, Varki NM and Varki A (1998) P-selectin deficiency attenuates tumor growth and metastasis. *Proc Natl Acad Sci U S A* 95:9325-30. doi: 10.1073/pnas.95.16.9325
46. Borsig L, Wong R, Feramisco J, Nadeau DR, Varki NM and Varki A (2001) Heparin and cancer revisited: mechanistic connections involving platelets, P-selectin, carcinoma mucins, and tumor metastasis. *Proc Natl Acad Sci U S A* 98:3352-7. doi: 10.1073/pnas.061615598
47. Alves CS, Burdick MM, Thomas SN, Pawar P and Konstantopoulos K (2008) The dual role of CD44 as a functional P-selectin ligand and fibrin receptor in colon carcinoma cell adhesion. *Am J Physiol Cell Physiol* 294:C907-16. doi: 10.1152/ajpcell.00463.2007
48. Felding-Habermann B, Habermann R, Saldivar E and Ruggeri ZM (1996) Role of beta3 integrins in melanoma cell adhesion to activated platelets under flow. *J Biol Chem* 271:5892-900. doi: 10.1074/jbc.271.10.5892
49. Suzuki-Inoue K, Kato Y, Inoue O, Kaneko MK, Mishima K, Yatomi Y, Yamazaki Y, Narimatsu H and Ozaki Y (2007) Involvement of the snake toxin receptor CLEC-2, in podoplanin-mediated platelet activation, by cancer cells. *J Biol Chem* 282:25993-6001. doi: 10.1074/jbc.M702327200
50. Yu LX, Yan L, Yang W, Wu FQ, Ling Y, Chen SZ, Tang L, Tan YX, Cao D, Wu MC, Yan HX and Wang HY (2014) Platelets promote tumour metastasis via interaction between TLR4 and tumour cell-released high-mobility group box1 protein. *Nat Commun* 5:5256. doi: 10.1038/ncomms6256
51. Gong L, Cai Y, Zhou X and Yang H (2012) Activated platelets interact with lung cancer cells through P-selectin glycoprotein ligand-1. *Pathol Oncol Res* 18:989-96. doi: 10.1007/s12253-012-9531-y
52. Aigner S, Ramos CL, Hafezi-Moghadam A, Lawrence MB, Friederichs J, Altevogt P and Ley K (1998) CD24 mediates rolling of breast carcinoma cells on P-selectin. *FASEB J* 12:1241-51. doi: 10.1096/fasebj.12.12.1241
53. Dimitroff CJ, Descheny L, Trujillo N, Kim R, Nguyen V, Huang W, Pienta KJ, Kutok JL and Rubin MA (2005) Identification of leukocyte E-selectin ligands, P-selectin glycoprotein ligand-1 and E-selectin ligand-1, on human metastatic prostate tumor cells. *Cancer Res* 65:5750-60. doi: 10.1158/0008-5472.CAN-04-4653
54. Nolo R, Herbrich S, Rao A, Zweidler-McKay P, Kannan S and Gopalakrishnan V (2017) Targeting P-selectin blocks neuroblastoma growth. *Oncotarget* 8:86657-86670. doi: 10.18632/oncotarget.21364
55. Vega FM, Colmenero-Repiso A, Gomez-Munoz MA, Rodriguez-Prieto I, Aguilar-Morante D, Ramirez G, Marquez C, Cabello R and Pardal R (2019) CD44-high neural crest stem-like cells are associated with tumour aggressiveness and poor survival in neuroblastoma tumours. *EBioMedicine* 49:82-95. doi: 10.1016/j.ebiom.2019.10.041
56. Wang CY, Huang CS, Yang YP, Liu CY, Liu YY, Wu WW, Lu KH, Chen KH, Chang YL, Lee SD and Lin HC (2019) The subpopulation of CD44-positive cells promoted tumorigenicity and metastatic ability in lung adenocarcinoma. *J Chin Med Assoc* 82:196-201. doi: 10.1097/JCMA.000000000000056
57. Xu H, Niu M, Yuan X, Wu K and Liu A (2020) CD44 as a tumor biomarker and therapeutic target. *Exp Hematol Oncol* 9:36. doi: 10.1186/s40164-020-00192-0

- 
58. Zanjani LS, Madjd Z, Abolhasani M, Rasti A, Fodstad O, Andersson Y and Asgari M (2018) Increased expression of CD44 is associated with more aggressive behavior in clear cell renal cell carcinoma. *Biomark Med* 12:45-61. doi: 10.2217/bmm-2017-0142

## Statutory Declaration

"I, Xiaotong Zhao, by personally signing this document in lieu of an oath, hereby affirm that I prepared the submitted dissertation on the topic "Platelet-based and platelet-mimicking modified human serum albumin submicron particles for tumor cell capture", "Thrombozyten-basierte und Thrombozyten nachahmende modifizierte Submikron-Partikel aus Humanserumalbumin zum Einfangen von Tumorzellen" independently and without the support of third parties, and that I used no other sources and aids than those stated.

All parts which are based on the publications or presentations of other authors, either in letter or in spirit, are specified as such in accordance with the citing guidelines. The sections on methodology (in particular regarding practical work, laboratory regulations, statistical processing) and results (in particular regarding figures, charts and tables) are exclusively my responsibility.

Furthermore, I declare that I have correctly marked all of the data, the analyses, and the conclusions generated from data obtained in collaboration with other persons, and that I have correctly marked my own contribution and the contributions of other persons (cf. declaration of contribution). I have correctly marked all texts or parts of texts that were generated in collaboration with other persons.

My contributions to any publications to this dissertation correspond to those stated in the below joint declaration made together with the supervisor. All publications created within the scope of the dissertation comply with the guidelines of the ICMJE (International Committee of Medical Journal Editors; <http://www.icmje.org>) on authorship. In addition, I declare that I shall comply with the regulations of Charité – Universitätsmedizin Berlin on ensuring good scientific practice.

I declare that I have not yet submitted this dissertation in identical or similar form to another Faculty.

The significance of this statutory declaration and the consequences of a false statutory declaration under criminal law (Sections 156, 161 of the German Criminal Code) are known to me."

Date

Signature

---

## Declaration of your own contribution to the publications

Xiaotong Zhao contributed the following to the below listed publications:

Publication 1: Zhao, Xiaotong, Radostina Georgieva, Pichayut Rerkshanandana, Moritz Hackmann, Lara-Elena Heil Olaizola, Maxine Müller-de Ahna, and Hans Bäumlner, Tumor Cell Capture Using Platelet-Based and Platelet-Mimicking Modified Human Serum Albumin Submicron Particles, International Journal of Molecular Sciences, 2022.

Contribution in detail:

- Carrying out all measurements
- Software
- Statistical Analysis
- Creation of all figures and table 1
- Writing—original draft preparation
- Revision (Partial Participation)

---

Signature, date and stamp of first supervising university professor / lecturer

---

Signature of doctoral candidate

## Excerpt from Journal Summary List

Publication 1: Tumor Cell Capture Using Platelet-Based and Platelet-Mimicking Modified Human Serum Albumin Submicron Particles

Journal Data Filtered By: **Selected JCR Year: 2021** Selected Editions: SCIE,SSCI  
 Selected Categories: **"BIOCHEMISTRY and MOLECULAR BIOLOGY"** Selected  
 Category Scheme: WoS  
**Gesamtanzahl: 296 Journale**

Rank	Full Journal Title	Total Cites	Journal Impact Factor	Eigenfaktor
1	NATURE MEDICINE	141,857	87.241	0.23255
2	CELL	362,236	66.850	0.53397
3	Molecular Cancer	32,250	41.444	0.03386
4	Signal Transduction and Targeted Therapy	11,026	38.104	0.01781
5	Annual Review of Biochemistry	25,139	27.258	0.01962
6	Molecular Plant	20,242	21.949	0.02339
7	MOLECULAR CELL	94,258	19.328	0.13937
8	NUCLEIC ACIDS RESEARCH	284,490	19.160	0.33755
9	NATURE STRUCTURAL & MOLECULAR BIOLOGY	33,999	18.361	0.04689
10	TRENDS IN MICROBIOLOGY	19,957	18.230	0.02015
11	CYTOKINE & GROWTH FACTOR REVIEWS	9,002	17.660	0.00625
12	MOLECULAR ASPECTS OF MEDICINE	8,986	16.337	0.00615
13	Nature Chemical Biology	31,125	16.174	0.04456
14	TRENDS IN MOLECULAR MEDICINE	14,585	15.272	0.01381
15	NATURAL PRODUCT REPORTS	14,564	15.111	0.01079
16	PROGRESS IN LIPID RESEARCH	7,982	14.673	0.00444
17	TRENDS IN BIOCHEMICAL SCIENCES	22,957	14.264	0.02170
18	EMBO JOURNAL	80,536	14.012	0.05438
19	MOLECULAR PSYCHIATRY	33,324	13.437	0.04914
20	Molecular Systems Biology	11,036	13.068	0.01483
21	EXPERIMENTAL AND MOLECULAR MEDICINE	12,199	12.153	0.01698

Rank	Full Journal Title	Total Cites	Journal Impact Factor	Eigenfaktor
22	PLANT CELL	67,319	12.085	0.02964
23	CELL DEATH AND DIFFERENTIATION	31,035	12.067	0.02639
24	BIOCHIMICA ET BIOPHYSICA ACTA-REVIEWS ON CANCER	8,255	11.414	0.00673
25	Cell Systems	8,047	11.091	0.03332
26	CURRENT BIOLOGY	85,124	10.900	0.10641
27	Redox Biology	20,557	10.787	0.02390
28	International Journal of Biological Sciences	14,100	10.750	0.01488
29	MATRIX BIOLOGY	9,415	10.447	0.00856
30	PLOS BIOLOGY	44,888	9.593	0.05920
31	Cell and Bioscience	4,564	9.584	0.00524
32	Science Signaling	17,426	9.517	0.02046
33	GENOME RESEARCH	51,169	9.438	0.05153
34	CELLULAR AND MOLECULAR LIFE SCIENCES	38,745	9.207	0.03204
35	Journal of Integrative Plant Biology	8,456	9.106	0.00730
36	EMBO REPORTS	21,705	9.071	0.02695
37	Cell Chemical Biology	6,651	9.039	0.01870
38	CURRENT OPINION IN CHEMICAL BIOLOGY	12,464	8.972	0.01277
39	MOLECULAR BIOLOGY AND EVOLUTION	67,311	8.800	0.07228
40	ONCOGENE	81,646	8.756	0.05014
41	CELLULAR & MOLECULAR BIOLOGY LETTERS	2,684	8.702	0.00250
42	CRITICAL REVIEWS IN BIOCHEMISTRY AND MOLECULAR BIOLOGY	5,108	8.697	0.00477
43	Molecular Ecology Resources	15,145	8.678	0.01553



Rank	Full Journal Title	Total Cites	Journal Impact Factor	Eigenfaktor
44	Plant Communications	743	8.625	0.00148
45	FREE RADICAL BIOLOGY AND MEDICINE	55,523	8.101	0.02824
46	INTERNATIONAL JOURNAL OF BIOLOGICAL MACROMOLECULES	112,372	8.025	0.09445
47	Biomedical Journal	2,388	7.892	0.00301
48	CURRENT OPINION IN STRUCTURAL BIOLOGY	13,407	7.786	0.01689
49	AMERICAN JOURNAL OF RESPIRATORY CELL AND MOLECULAR BIOLOGY	16,259	7.748	0.01386
50	Antioxidants	21,453	7.675	0.01946
51	EXPERT REVIEWS IN MOLECULAR MEDICINE	2,282	7.615	0.00062
52	Reviews of Physiology Biochemistry and Pharmacology	920	7.500	0.00043
53	ANTIOXIDANTS & REDOX SIGNALING	29,117	7.468	0.01390
54	Essays in Biochemistry	4,569	7.258	0.00691
55	Genes & Diseases	2,732	7.243	0.00322
56	Open Biology	5,227	7.124	0.00994
57	PROTEIN SCIENCE	18,673	6.993	0.02822
58	BIOMACROMOLECULES	46,963	6.978	0.02347
59	JOURNAL OF PHOTOCHEMISTRY AND PHOTOBIOLOGY B-BIOLOGY	18,610	6.814	0.01229
60	JOURNAL OF LIPID RESEARCH	29,128	6.676	0.01485
61	BIOCHIMICA ET BIOPHYSICA ACTA-MOLECULAR BASIS OF DISEASE	22,719	6.633	0.01820
62	MOLECULAR ECOLOGY	45,664	6.622	0.03311
63	AMYLOID-JOURNAL OF PROTEIN FOLDING DISORDERS	2,335	6.571	0.00312

Rank	Full Journal Title	Total Cites	Journal Impact Factor	Eigenfaktor
64	BIOFACTORS	5,614	6.438	0.00307
65	International Review of Cell and Molecular Biology	3,388	6.420	0.00314
66	MOLECULAR MEDICINE	7,039	6.376	0.00402
67	Food & Function	27,282	6.317	0.02290
68	Biochimica et Biophysica Acta- Gene Regulatory Mechanisms	8,926	6.304	0.00707
69	<b>INTERNATIONAL JOURNAL OF MOLECULAR SCIENCES</b>	<b>211,517</b>	<b>6.208</b>	<b>0.24907</b>
70	Computational and Structural Biotechnology Journal	6,436	6.155	0.00945
71	JOURNAL OF MOLECULAR BIOLOGY	66,672	6.151	0.03581
72	JOURNAL OF NUTRITIONAL BIOCHEMISTRY	15,277	6.117	0.00837
73	Frontiers in Molecular Biosciences	6,864	6.113	0.01068
74	BIOCONJUGATE CHEMISTRY	19,624	6.069	0.01508
75	Biomolecules	21,742	6.064	0.02602
76	GLYCOBIOLOGY	10,212	5.954	0.00650
77	STRUCTURE	17,734	5.871	0.01779
78	MACROMOLECULAR BIOSCIENCE	9,240	5.859	0.00565
79	FASEB JOURNAL	59,831	5.834	0.04452
80	ACS Chemical Neuroscience	12,168	5.780	0.01655
81	BIOELECTROCHEMISTRY	7,093	5.760	0.00463
82	JOURNAL OF ENZYME INHIBITION AND MEDICINAL CHEMISTRY	8,156	5.756	0.00580
83	Journal of Genetics and Genomics	3,129	5.723	0.00327
84	Acta Crystallographica Section D-Structural Biology	23,006	5.699	0.02041
85	REDOX REPORT	2,247	5.696	0.00082

# Printing copy(s) of the publication(s)



## Article

# Tumor Cell Capture Using Platelet-Based and Platelet-Mimicking Modified Human Serum Albumin Submicron Particles

Xiaotong Zhao <sup>1</sup>, Radostina Georgieva <sup>1,2</sup> , Pichayut Rerkshanandana <sup>1</sup>, Moritz Hackmann <sup>1</sup>,  
Lara-Elena Heil Olaizola <sup>1</sup> , Maxine Müller-de Ahna <sup>1</sup> and Hans Bäuml <sup>1,\*</sup>

<sup>1</sup> Institute of Transfusion Medicine, Charité-Universitätsmedizin Berlin, 10117 Berlin, Germany

<sup>2</sup> Department of Medical Physics, Biophysics and Radiology, Medical Faculty, Trakia University, 6000 Stara Zagora, Bulgaria

\* Correspondence: hans.baemler@charite.de; Tel.: +49-30-450525131



**Citation:** Zhao, X.; Georgieva, R.; Rerkshanandana, P.; Hackmann, M.; Heil Olaizola, L.-E.; Müller-de Ahna, M.; Bäuml, H. Tumor Cell Capture Using Platelet-Based and Platelet-Mimicking Modified Human Serum Albumin Submicron Particles. *Int. J. Mol. Sci.* **2022**, *23*, 14277. <https://doi.org/10.3390/ijms232214277>

Academic Editors: Wen-Chiuan Tsai, Ying Chen and Chen-Liang Tsai

Received: 11 October 2022

Accepted: 14 November 2022

Published: 18 November 2022

**Publisher's Note:** MDPI stays neutral with regard to jurisdictional claims in published maps and institutional affiliations.



**Copyright:** © 2022 by the authors. Licensee MDPI, Basel, Switzerland. This article is an open access article distributed under the terms and conditions of the Creative Commons Attribution (CC BY) license (<https://creativecommons.org/licenses/by/4.0/>).

**Abstract:** The co-localization of platelets and tumor cells in hematogenous metastases has long been recognized. Interactions between platelets and circulating tumor cells (CTCs) contribute to tumor cell survival and migration via the vasculature into other tissues. Taking advantage of the interactions between platelets and tumor cells, two schemes, direct and indirect, were proposed to target the modified human serum albumin submicron particles (HSA-MPs) towards tumor cells. HSA-MPs were constructed by the Co-precipitation–Crosslinking–Dissolution (CCD) method. The anti-CD41 antibody or CD62P protein was linked to the HSA-MPs separately via 1-ethyl-3-(3-dimethyl aminopropyl) carbodiimide hydrochloride (EDC) and N-hydroxysuccinimide (NHS) EDC/NHS chemistry. The size of modified HSA-MPs was measured at approximately 1  $\mu\text{m}$ , and the zeta potential was around  $-24$  mV. Anti-CD41-HSA-MPs adhered to platelets as shown by flowcytometry and confocal laser scanning microscopy. In vitro, we confirmed the adhesion of platelets to tumor lung carcinoma cells A549 under shearing conditions. Higher cellular uptake of anti-CD41-HSA-MPs in A549 cells was found in the presence of activated platelets, suggesting that activated platelets can mediate the uptake of these particles. RNA-seq data in the Cancer Cell Lineage Encyclopedia (CCLE) and The Cancer Genome Atlas (TCGA) database showed the expression of CD62P ligands in different types of cancers. Compared to the non-targeted system, CD62P-HSA-MPs were found to have higher cellular uptake in A549 cells. Our results suggest that the platelet-based and platelet-mimicking modified HSA-MPs could be promising options for tracking metastatic cancer.

**Keywords:** human serum albumin (HSA); platelets; circulating tumor cells; submicron particles; adhesion

## 1. Introduction

Hematogenous metastasis, a multi-step and complex process, is responsible for most cancer-related deaths [1]. Cancer cell spread begins when cancer cells acquire invasive potential, facilitating their escape from the primary tumor. The epithelial to mesenchymal transition (EMT) of tumor cells is considered to be the main driving force for cancer cell spread and CTC production [2–4]. After entering the vasculature, most CTCs die due to the hemodynamic forces, anoikis, and the immune system [5]. The surviving tumor cells exit the vasculature through endothelial cells [6].

Platelets can be activated by tumor cells and subsequently attach to the CTCs as a protective shield to help the CTCs survive in circulation [7–9]. The ATP released by tumor cell-activated platelets opens the endothelium barrier, allowing tumor cells to migrate transendothelially and, thereby, enhance cancer cell extravasation [10]. During the past decades, many studies have revealed receptor–ligand interactions between activated platelets and tumor cells, such as CD62P (P-selectin) and P-selectin ligands [11,12]. These

findings lay the groundwork for the use of platelet-mediated delivery technology to treat cancer diseases.

In view of the important role of platelets in tumor pathogenesis, there is a growing interest in utilizing platelets to develop efficient anti-tumor therapeutic approaches. For instance, anti-PD-L1 antibodies were linked to the surface of platelets to treat breast carcinomas and leukemia [13,14]; covering particles with platelet membranes is another strategy that has been discussed [15,16]. However, platelets are easy to be activated and distorted during the manufacture of platelet carriers *in vitro* and increase the probability of forming a thrombus after re-transfusion. Platelets, similar to red blood cells, face restrictions in proper storage and contamination. Long-term maintenance of the biological functions of modified platelets is difficult. Furthermore, increased exogenous platelet numbers can result in tumor-related thrombosis and promote tumor progression [17]. Therefore, drug-loaded autologous platelets can be considered the ideal medium to deliver drugs to tumor cells. Mimicking some functions of platelets by protein particles could also be an excellent strategy to avoid the disadvantages caused by the exogenous platelet.

Human serum albumin (HSA), the most abundant plasma protein, has been used as a multifunctional drug delivery platform in the biomedical field. The extensive research and application of HSA are attributed to its good biocompatibility, biodegradability, non-toxicity, and non-immunogenicity [18]. Some anticancer medications, including paclitaxel, Methotrexate, and 5-fluorouracil, are used successfully when coupled with albumin [19–21]. Abraxane<sup>®</sup> (nanoparticle albumin-bound paclitaxel) for breast cancer treatment is already in clinical application [22,23]. Although HSA possesses great biological properties as a drug carrier, further research is still required to improve its selective targeting capability. Our team has developed a successful technique called Co-precipitation–Crosslinking–Dissolution (CCD) for the fabrication of protein particles [24–26]. Human serum albumin submicron particles (HSA-MPs) produced by this technique were already used as a vehicle platform successfully loaded with riboflavin and Doxorubicin [27,28].

In this study, we explored two drug delivery strategies that take advantage of the adhesion ability of platelets to CTCs (Figure 1A). (1) CD41, also known as GpIIb, is a cell-surface protein expressed at high levels on platelets. The anti-CD41 antibody-modified HSA-MPs are designed to trail tumor cells by hitchhiking on the platelet. (Figure 1B). (2) The mechanism of platelet aggregation around tumor cells includes the binding of biomolecules such as CD62P, which belongs to the selectin family. CD62P translocates to the platelet surface when platelets are activated, mediating the adhesion of platelets to the endothelial cells, leukocytes, and tumor cells [29,30]. We revealed the expression of common ligands for CD62P, including CD44, SELPLG, and CD24 [31], in pan-cancer analysis using TCGA and CCLE datasets. The CD62P enabled the HSA-MPs to specifically bind to the upregulated receptors on the surface of tumor cells. The platelet-mimicking particles with platelet-specific protein modifications, CD62P-HSA-MPs, were constructed to directly target tumor cells specifically (Figure 1C).

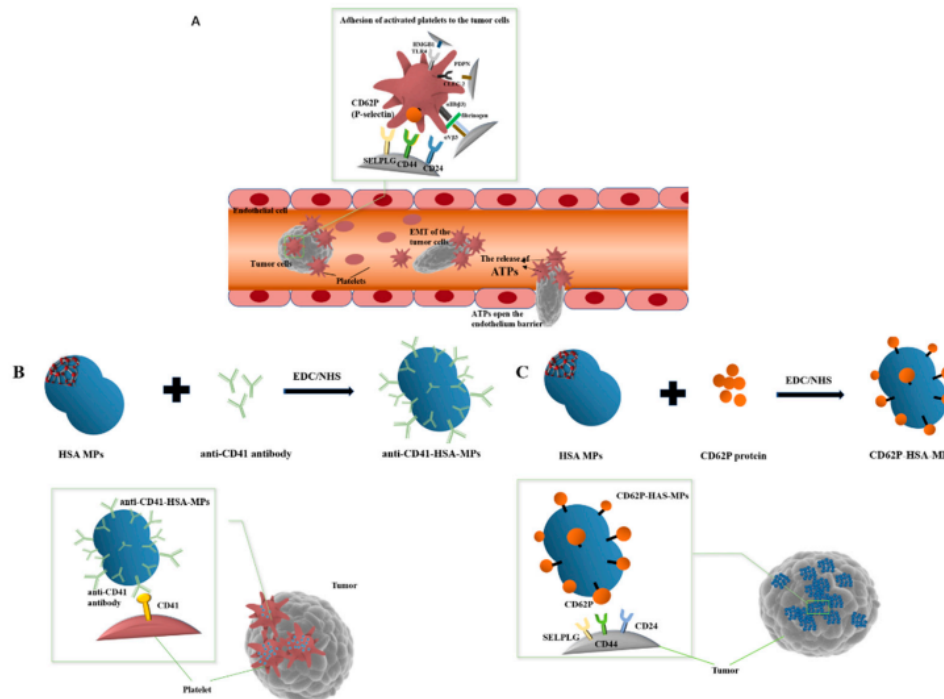


**Figure 1.** Schematic of targeting strategies. (A). Schematic of the circulating tumor cell captured by activated platelets in vivo, adhering and escaping through gaps of the endothelium. (B). Anti-CD41-HSA-MPs hitchhiked on platelets to target circulating tumor cells indirectly. (C). CD62P-HSA-MPs target a tumor cell directly mediated by the CD62P on the surface of the HSA-MPs.

## 2. Results and Discussion

### 2.1. Characterization of Anti-CD41-HSA-MPs and CD62P-HSA-MPs

The size, polydispersity index (PDI), and zeta potential of anti-CD41-HSA-MPs and CD62P-HSA-MPs were analyzed by Zetasizer Nano ZS. Both particles showed a submicron size ranging from 0.9 to 1  $\mu\text{m}$ , and the zeta potentials were around  $-24$  mV (Table 1). When compared to reported HSA-MPs manufactured using the CCD method, the modified HSA-MPs' sizes increased slightly [28,32,33].

**Table 1.** Particle size and zeta potential.

Sample	Average Size (nm)	Polydispersity Index (PDI)	Zeta Potential (mV)	Conductivity (mS/cm)
anti-CD41-HSA-MPs	952 $\pm$ 41	0.24 $\pm$ 0.03	$-25 \pm 1$	1.3 $\pm$ 0.1
CD62P-HSA-MPs	974 $\pm$ 15	0.26 $\pm$ 0.11	$-24 \pm 2$	1.4 $\pm$ 0.1
HSA-MPs	847 $\pm$ 24	0.26 $\pm$ 0.11	$-26 \pm 1$	1.3 $\pm$ 0.1

### 2.2. Platelet Adhesion to the A549 Tumor Cells In Vitro

The adhesion ability of activated platelets to the CTCs was an essential basis in this study. Platelets were isolated from healthy humans and activated under shearing conditions using a rheometer to verify the adhesion between activated platelets and A549 cells. As shown In Figure 2A–C, the fluorescence intensity quantified by a flow cytometer in the APC channel also showed similar results. The percentage of A549 cells with APC anti-CD41 antibody-labeled or Alexa 647 anti-CD62P antibody-labeled platelets were  $65 \pm 11\%$  and



$50 \pm 8\%$ , respectively. The fluorescent images (Figure 2D) showed the adhesion of the platelet to the A549 tumor cell under the fluorescence microscope. The platelets were labeled with anti-CD41 antibody (red fluorescence) and the activated ones were labeled with Alexa 488 anti-CD62P antibody (green fluorescence). Many more platelets were labeled with the APC anti-CD41 antibody than with the Alexa 488 anti-CD62P antibody, probably due to the lower number of activated platelets and the fact that CD62P on the platelets itself acts as a binding site to the A549 cells.

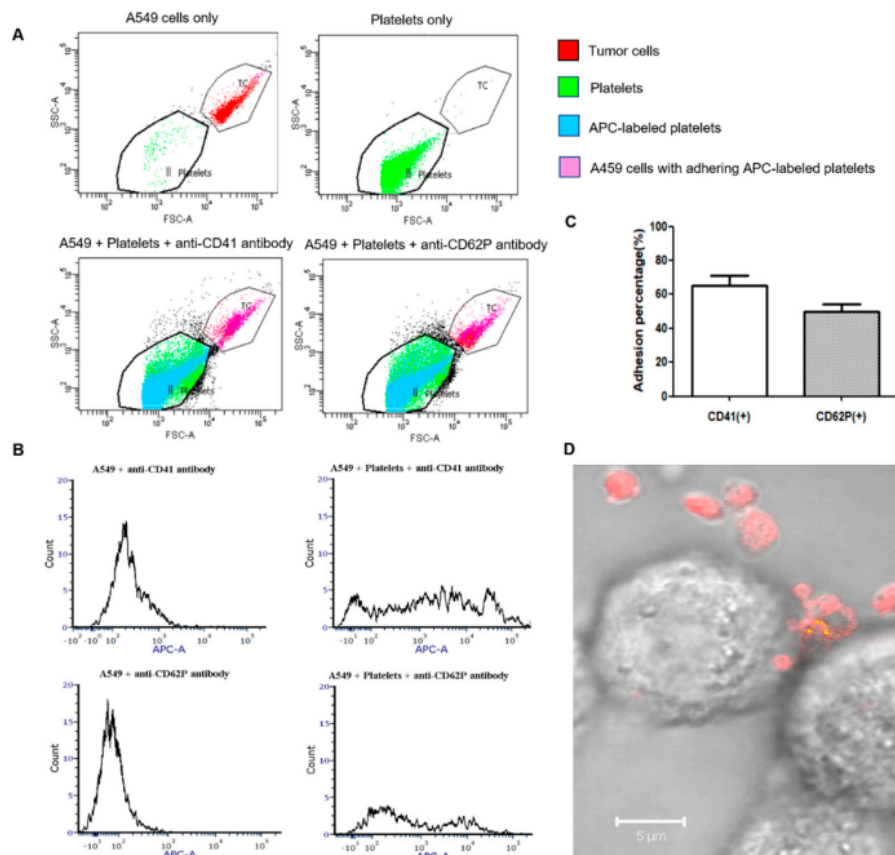


**Figure 2.** Adhesion of platelets to A549 cells under shearing conditions analyzed by flow cytometry and confocal laser scanning microscopy. (A) Dot plots of A549 cells, platelets, A549 cells + platelets + APC anti-CD41 antibody, and A549 + platelets + Alexa 647 anti-CD62P antibody (250 platelets/tumor cell). The platelets were labeled with APC anti-CD41 antibody or Alexa 647 anti-CD62P antibody separately. The A549 cell and platelet populations were identified by their forward scatter (FSC) and side scatter (SSC). (B) Histograms of the fluorescence intensity in the tumor cell population for A549 cells + APC anti-CD41 antibody (control), A549 cells + Platelets + APC anti-CD41 antibody, A549 cells + Alexa 647 anti-CD62P antibody (control), and A549 cells + Platelets + Alexa 647 anti-CD62P antibody. (C) Percentage of A549 cells with adhering platelets labeled with APC anti-CD41 antibody or Alexa 647 anti-CD62P antibody. (D) Representative image of platelets adhering to A549 tumor cell as observed under the confocal laser scanning microscope. The platelets were labeled with APC anti-CD41 antibody (red fluorescence) and Alexa 488 anti-CD62P antibody (green fluorescence). The yellow color represents overlapped red and green fluorescence.

Platelets are one of the first circulating cells that CTCs encounter during metastasis. Most CTCs only survive in circulation for a short time before being trapped in the endothelial cells of blood vessels or eliminated by the immune system. Under shear stress, approximately 0.1% of CTCs are physically protected by the platelet-rich thrombi surrounding them [34,35]. Activated platelets cover the CTCs as “coats” and prevent cancer cells from being eliminated, promoting cancer progression. The expression of four platelet activation markers, including CD62P, GPIIb/IIIa, lysosomal glycoprotein, and phosphatidylserine, significantly increases following transitory exposure to higher shear strain rates [36]. In vitro, we confirmed the adhesion of platelets to the A549 cells under shearing conditions through flow cytometry and microscopy. This process can be explained by the activation of platelets under shear stress and the translocation of the tumor cell receptors, such as CD62P, to the activated platelet surface, which mediates the adhesion of platelets and tumor cells.

### 2.3. Anti-CD41-HSA-MP Adhesion to Platelets In Vitro

The results of the adhesion experiments performed by incubating platelets with the FITC-labeled HSA-MPs (20 particles/platelets) for 30 min are summarized in Figure 3. The flow cytometry results showed that the adhesion percentage of anti-CD41-FITC-HSA-MPs to the platelets was slightly higher than that of non-modified control FITC-HSA-MPs (Figure 3B). The higher mean fluorescence intensity of platelets in the FITC channel (Figure 3C) and typical fluorescence microscope images (Figure 3D) indicated that more anti-CD41-HSA-MPs adhere to the A549 cells than control HSA-MPs.

It should be noted that the number of activated platelets is small. The majority of platelets in natural blood circulation are resting platelets. Platelets can be activated in large numbers under certain conditions, such as disease or injury. CD41, a cell-surface protein, is highly expressed on platelets and is used as a biomarker for platelets. It is a good choice to regard CD41 as a platelet-binding target for HSA-MPs. It is more efficient to use the anti-CD41-HSA-MPs hitchhiking on platelets, which could be activated under pathological conditions, than hitchhike on activated platelets only.

### 2.4. Cellular Uptake of Anti-CD41-HSA-MPs in A549 Cells Pre-Incubated with Platelets

Gp60, SPARC, Gp18, and Gp30 are the major albumin-binding proteins that are overexpressed in multiple tumors and the primary mechanism responsible for the uptake of albumin in tumors, a process that includes transcytosis through endothelium and endocytosis in tumor cells [37–39]. Because of the expression of albumin-binding proteins on the cell surface, the A549 cell line is a widely used tool for studying the interaction of albumin particles and tumor cells [27,33,40]. It has already been shown that the HSA-MPs can bind to and be endocytosed by A549 cells [27].

A549 cells were pre-incubated with arachidonic acid-activated platelets for 30 min and then FITC-labeled anti-CD41-HSA-MPs or HSA-MPs were added and the samples were incubated for 24 h. The fluorescence intensity analyzed by the flow cytometer (Figure 4) showed a significantly higher cellular uptake of anti-CD41-HSA-MPs than that of HSA-MPs in the presence of platelets. In the absence of the platelets, the cellular uptake of anti-CD41-HSA-MPs was reduced and had no difference with HSA-MPs. Measurement of fluorescence using flow cytometry allowed us to determine the A549 cells with internalized or adherent particles. The fully internalized particles were then retained by quenching the fluorescence of the remaining extracellular particles using Trypan blue. The cellular uptake percentage and MFI value decreased in all groups after quenching. However, the cellular uptake of anti-CD41-HSA-MPs in the presence of platelets was still significantly higher than that of HSA-MPs, which means that the platelet-adhering anti-CD41-HSA-MPs could be internalized more efficiently by A549 cells than the HSA-MPs in the presence of activated platelets.

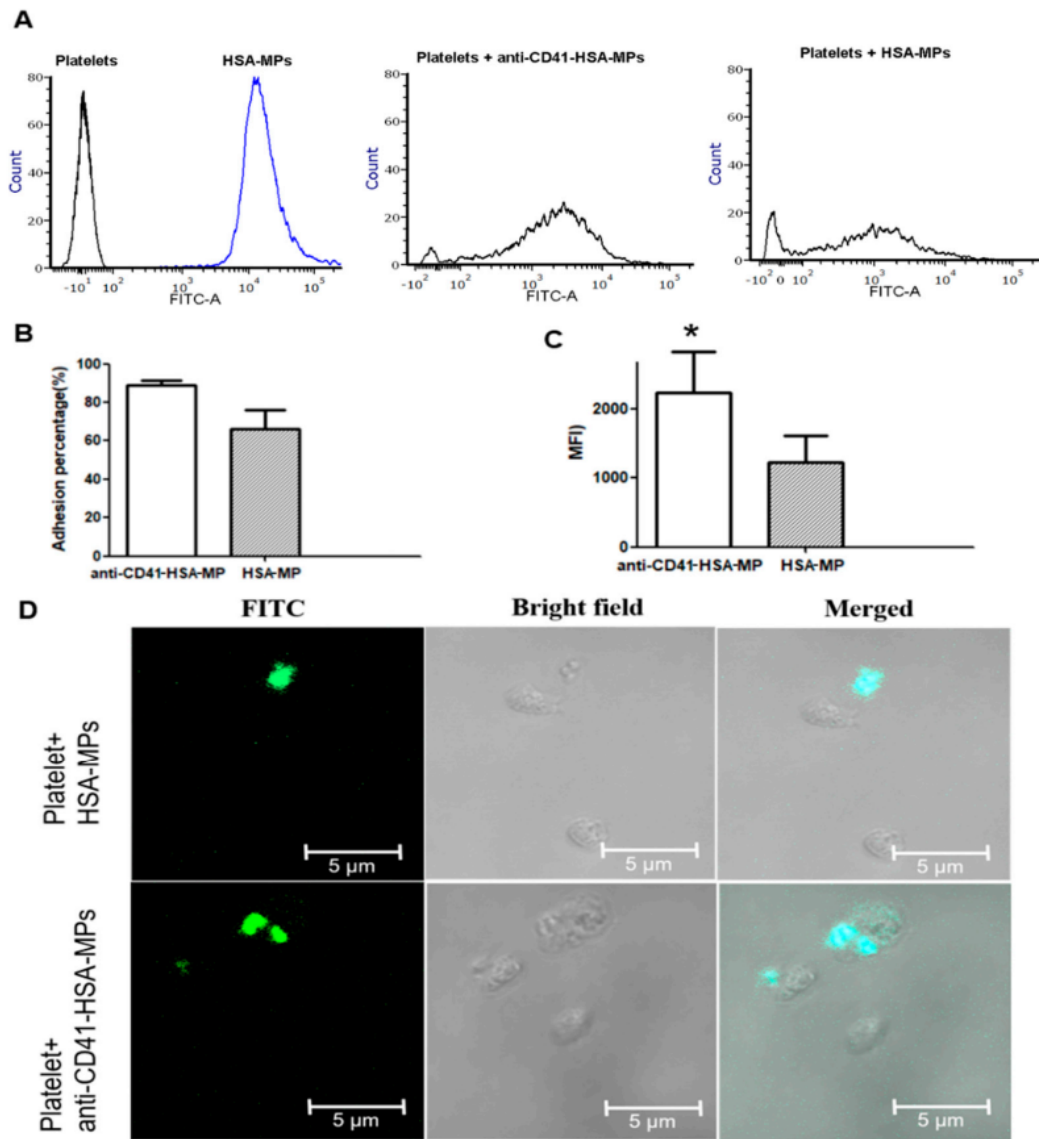


**Figure 3.** Adhesion of anti-CD41-HSA-MPs to platelets (A). Flow cytometry histograms of the fluorescence intensity in the platelet or FITC-HSA-MP populations (black line: platelets only; blue line: FITC-HSA-MPs only), and in the populations of platelets incubated with FITC-HSA-MPs or platelets incubated with anti-CD41-FITC-HSA-MPs, respectively. (B). Percentage of platelets with adhered FITC-HSA-MPs or anti-CD41-FITC-HSA-MPs. (C). Mean fluorescent intensity (MFI) values of the platelet population in the FITC channel. \*  $p < 0.05$ . (D). Representative confocal laser scanning microscopy images of HSA-MPs and anti-CD41-HSA-MPs with platelets.



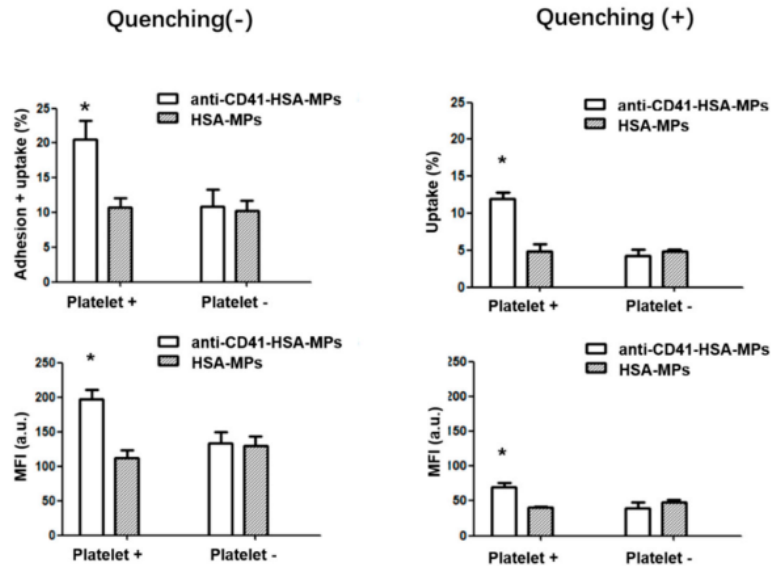


**Figure 4.** Adhesion vs. cellular uptake of anti-CD41-HSA-MPs and HSA-MPs in A549 cells analyzed by flow cytometry with or without pre-incubation with activated platelets. Adhering particles are excluded by quenching with Trypan blue. The upper graphs show the percentage of events in the A549 cell population with enhanced fluorescence in the FITC channel. The lower graphs show the corresponding Mean Fluorescence Intensities. \*  $p < 0.05$ .

The results could be explained by platelets serving as a connection between anti-CD41-HSA-MPs and tumor cells. The activated platelets could adhere to tumor cells. Hitchhiking of HSA-MPs on platelets via anti-CD41 promotes the possibility of particle/tumor cell interaction due to the adherence of activated platelets to the cells. The internalization of the anti-CD41-HSA-MPs is then further supported through the albumin-binding receptor proteins on the surface of the tumor cells. This means that the anti-CD41-HSA-MPs could detect the tumor cells with the help of platelets in the circulation and could be used to deliver anticancer drugs, avoiding an ex vivo treatment of platelets.

#### 2.5. Cellular Uptake of CD62P-HSA-MPs in A549 Cells

A549 cells were incubated with FITC-labeled CD62P-HSA-MPs or HSA-MPs for 24 h, and the resulting fluorescence per cell was measured by flow cytometry after quenching or not. The HSA-MPs served as a control. The cellular uptake percentage and MFI in the CD62P-HSA-MP group were both higher than those in the HSA-MP group with and without quenching (Figure 5). This means that CD62P-HSA-MPs could be internalized more efficiently than the HSA-MPs by the A549 cells.

The CD62P-HSA-MPs are expected to be used to specifically affect the formation of platelet “coat” through competitive inhibition. These results help us further in the next step to develop a targeted and sustained drug delivery system. We realize that the interactions between targeted drug carriers and cancer cells may differ in a physiological experimental environment, such as in the presence of other natural blood cells. It may be necessary to perform in vivo tests in the future to explore the effects of the modified HSA-MPs in the circulation.

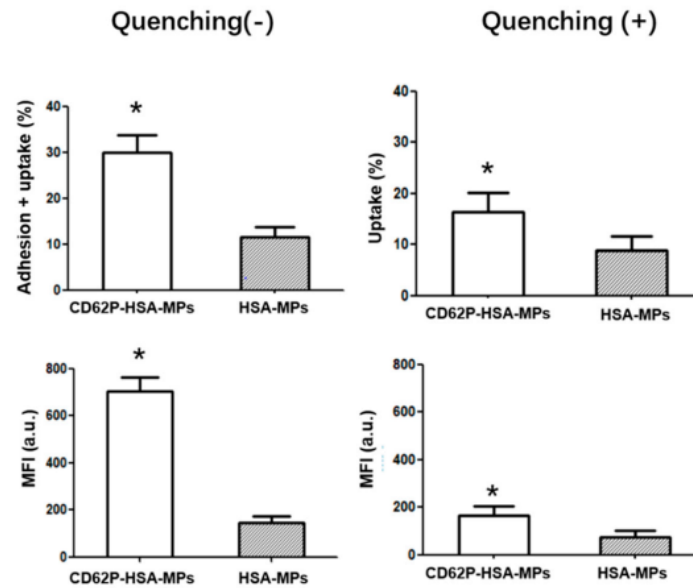


**Figure 5.** Adhesion vs. cellular uptake of anti-CD62P-HSA-MPs and HSA-MPs in A549 cells analyzed by flow cytometry. Adhering particles are excluded by quenching with Trypan blue. Upper graphs show the percentage of events in the A549 cell population with enhanced fluorescence in the FITC channel. Lower graphs show the corresponding Mean Fluorescence Intensities. \*  $p < 0.05$ .

#### 2.6. The Expression Level of the Ligands to CD62P in CCLE and TCGA Databases

CD62P has been suggested as an essential molecule for the adhesion of platelets to tumor cells. CD62P ligands,  $\alpha_{IIb}\beta_3$  integrins–fibrinogen– $\alpha_V\beta_3$ , CLEC-2–PDPN, and TLR4–HMGB1 are other receptor–ligand interactions that support the activation of platelets and aggregation on tumor cells [41–43]. Compared to the other receptor–ligand interactions, the related research on CD62P and its ligands is more extensive and in-depth. Gong et al. demonstrated that CD62P expression on platelets in the peripheral blood of cancer patients was significantly higher than that in healthy patients [44]. Moreover, different kinds of CD62P ligands, such as CD44, SELPLG, and CD24, have been shown overexpressed in different human carcinomas [31,45–50]. In practical drug delivery applications, tumor cells should be compared with noncancerous cells with low platelet-binding capacity when evaluating the platelet-mimicking carriers targeting tumor cells. In this instance, a high level of targeted binding with tumor cells is conducive to the use of a carrier system.

RNA-seq data in the CCLE database showed that CD44, SELPLG, and CD24 were expressed in almost all types of tumors (Figure 6A). Then, we retrieved the differential expression pattern of CD44, SELPLG, and CD24 in 33 types of cancers and adjacent normal tissues from the TCGA database. Our analysis showed that the expression of ligands was significantly higher in 17 cancers out of 33 types of cancers (Figure 6B). The above results provided a basis for the application of the CD62P-based albumin tumor-targeting carrier in tracking different types of CTCs.

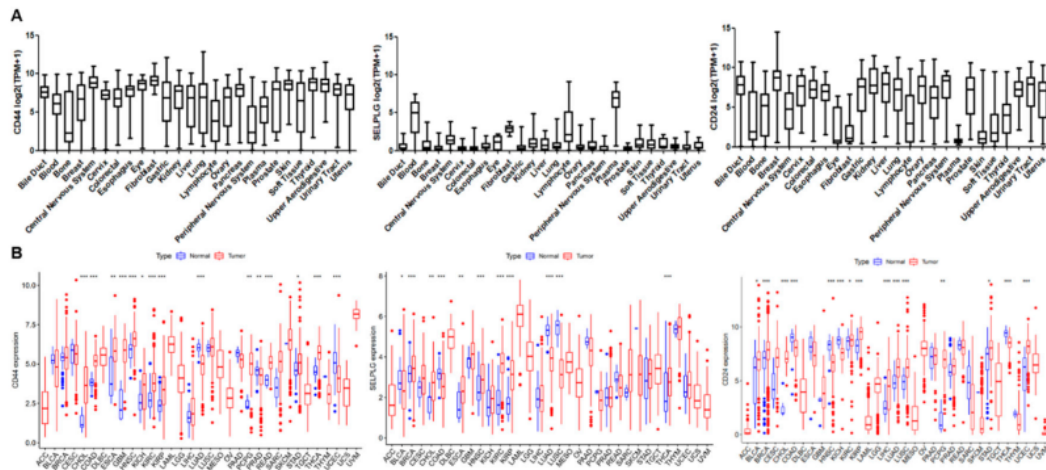


**Figure 6.** The mRNA expression of the ligands to the CD62P in the CCLE and TCGA database. (A) The mRNA expression levels of CD44, SELPLG, and CD24 in multiple cancer cell lines in the CCLE database. (B) The mRNA expression levels of CD44, SELPLG, and CD24 in multiple cancer types and corresponding normal tissues in TCGA database. \*  $p < 0.05$ ; \*\*  $p < 0.01$ ; \*\*\*  $p < 0.001$ .

### 3. Materials and Methods

#### 3.1. Materials

APC anti-CD41 antibody, Alexa 647 anti-CD62P antibody, and Alexa 488 anti-CD62P antibody were purchased from BioLegend (San Diego, CA, USA). Anti-CD41 antibody (Biotin) was purchased from Antibodies.com (Cambridge, UK). CD62P protein was purchased from Sino Biological (Eschborn, Germany). Human serum albumin solution (200 g/L HSA, 145 mM NaCl) was from Grifols (Frankfurt, Germany). Dimethyl sulfoxide (DMSO) and sodium hydroxide (NaOH) were purchased from Carl Roth (Karlsruhe, Germany). Ethylene diamine tetra-acetic acid (EDTA) was purchased from Fluka (Buchs, Switzerland). Glutaraldehyde (GA), sodium carbonate ( $\text{Na}_2\text{CO}_3$ ), magnesium chloride ( $\text{MnCl}_2$ ), phosphate-buffered saline (PBS), glycine, sodium borohydride ( $\text{NaBH}_4$ ), and fluorescein isothiocyanate (FITC) were purchased from Sigma-Aldrich (Munich, Germany). 1-Ethyl-3-(3-dimethyl aminopropyl) carbodiimide hydrochloride (EDC), 2-(N-morpholino)ethanesulfonic acid (MES), and (hydroxymethyl) aminomethane (Tris) were purchased from Thermo Scientific (Rockford, IL, USA). N-Hydroxysuccinimid (NHS) was purchased from Fluka (St. Louis, MO, USA). Arachidonic acid was purchased from Møláb (Langenfeld, German).

#### 3.2. Preparation of Human Serum Albumin Particles (HSA-MPs)

The HSA-MPs were fabricated by the CCD technique [24,27,28]. Briefly, equal volumes of 0.125 M  $\text{MnCl}_2$  with 10 mg/mL HSA and 0.125 M  $\text{Na}_2\text{CO}_3$  were quickly added under stirring for 30 s at room temperature to produce HSA- $\text{MnCO}_3$ -MPs. According to the experimental needs, 0.025 mg/mL FITC in DMSO was added in the previous step. Then, 0.05% HSA solution was added to the suspension and incubated for an additional 5 min under stirring to prevent agglomeration of the particles. We then washed the HSA- $\text{MnCO}_3$ -MPs with 0.9% NaCl three times (3000 g, 5 min). The suspension was then cross-linked with 0.1% glutaraldehyde (GA) for 1 h at room temperature. Next, it was incubated with 0.08 M glycine and 0.625 mg/mL  $\text{NaBH}_4$  for 30 min to quench the remaining GA. Finally, 0.25 M EDTA was used to dissolve the  $\text{MnCO}_3$  templates (30 min). The obtained particles were washed three times (1000 g, 10 min) and stored in 0.9% NaCl for further use.

### 3.3. Preparation of Anti-CD41-HSA-MPs and CD62P-HSA-MPs

Anti-CD41 antibody was coupled to HSA-MPs through 1-ethyl-3-(3-dimethyl amino-propyl) carbodiimide hydrochloride (EDC) and N-hydroxysuccinimide (NHS) EDC/NHS chemistry. First, HSA-MPs were repeatedly washed with activation buffer (50 mM MES buffer, PH 6). Then, 4.8 mM EDC and 48 mM NHS were simultaneously added to a 0.1% HSA-MP solution. This mixture was incubated at room temperature for 30 min. Afterwards, the anti-CD41 antibody was added to reach a 10 µg/mL concentration. We then mixed the solution well and then allowed the reaction to proceed for 2.5 h. Quenching was performed by adding glycine to a final 4 mg/mL concentration. Finally, the solution was washed with blocking buffer (50 mM Tris pH 8 and 0.5% HSA), and the final anti-CD41-HSA-MPs were stored in the blocking buffer. The same method was used during the preparation of CD62P-HSA-MPs (Figure 7).

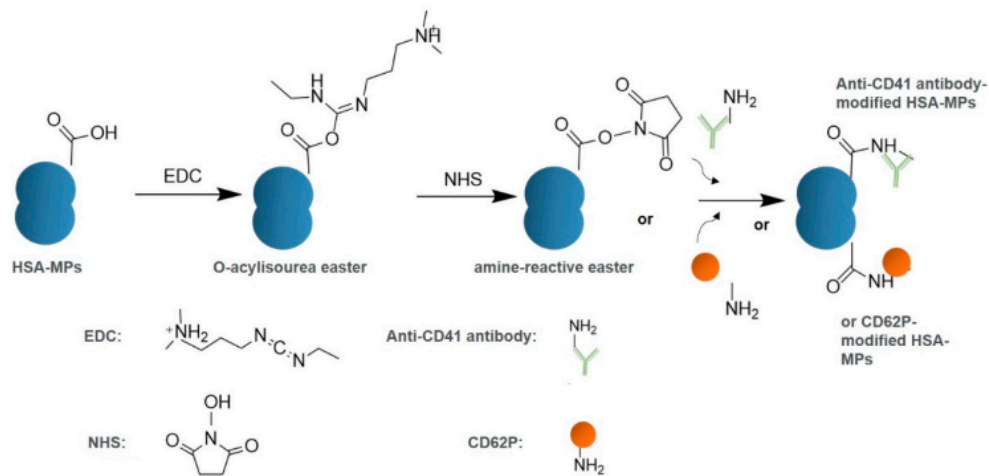


**Figure 7.** Scheme of modification on the surface of HSA-MPs by EDC/NHS method.

### 3.4. Particle Characterization

The size, polydispersity index (PDI), and zeta potential of the anti-CD41-HSA-MPs and CD62P-HSA-MPs in 10 mM NaCl were measured by Dynamic Light Scattering (Zetasizer Nano ZS, Malvern Instruments Ltd., Malvern, UK). The results were expressed as mean  $\pm$  standard deviation.

### 3.5. Cell Culture

The human pulmonary adenocarcinoma cell line A549 was a gift from Prof. Sergio Moya (CIC biomaGUNE, San Sebastian, Spain). The A549 cell line was cultured in RPMI 1640 medium (Corning, New York, NY, USA) supplemented with 10% FBS (Biochrom, Berlin, Germany) and 1% penicillin–streptomycin. The cells were incubated at 37 °C and 5% CO<sub>2</sub> in the incubator (Thermo Scientific, Waltham, MA, USA).

### 3.6. Preparation of Platelets

Blood samples from healthy human volunteers (EA1/110/21—Ethics committee Charité) were collected into 0.105 M Na<sub>3</sub> citrate tubes (366575, BD Vacutainer). The platelet-rich plasma (PRP) was isolated by centrifugation from whole blood (150  $\times$  g, 15 min).

### 3.7. Adhesion of Platelets to Tumor Cells under Shearing Condition

Under normal hematological circumstances, the platelets activated in response to shear stress [51]. The high shear rates were able to induce platelet activation [36]. After



trypsinization, A549 cells were incubated in PRP (tumor/platelet = 1/250) for 30 min under  $3000 \text{ s}^{-1}$  shear rate in a high-performance rheometer (Physica MCR 301, Anton Paar, Graz, Austria) at  $37^\circ\text{C}$ . The platelets were marked with APC anti-CD41 antibody, Alexa 647 anti-CD62P antibody, or Alexa 488 anti-CD62P antibody. The percentage of cells with the adhesion of particles and the mean fluorescence intensity (MFI) of A549 cells were quantified by flow cytometry in the APC channel (BD FACS Canto II, Franklin Lakes, NJ, USA). The samples were also observed under a fluorescence microscope (CLSM Zeiss LSM 510 meta, Zeiss MicroImaging GmbH, Jena, Germany).

### 3.8. Adhesion of Anti-CD41-HSA-MPs to Platelets

The PRP and anti-CD41-FITC-HSA-MP suspensions (20 particles/platelet) were mixed in the EP tube and incubated on the rotator at  $37^\circ\text{C}$ . After 30 min of coincubation, the samples were fixed with 4% paraformaldehyde in PBS. After that, the adhesion of anti-CD41-FITC-HSA-MPs to platelets was analyzed using flow cytometry in the FITC channel and observed under the fluorescence microscope

### 3.9. Cellular Uptake Assay

In 24-well plates, A549 cells were seeded and incubated overnight. The medium was then replaced with fresh serum-free medium containing FITC-labeled HAS-MPs, anti-CD41-HAS-MPs, or CD62P-HSA-MPs (MPs/A549 = 5000/1) and co-incubated for 24 h. The activated platelets were prepared by incubating with arachidonic acid (5 mg/mL) for 30 min at  $37^\circ\text{C}$ . To investigate the effect of activated platelets on cellular uptake, we pre-incubated A549 cells with arachidonic acid-activated platelets for 30 min before incubation with HAS-MPs or anti-CD41-HSA-MPs for an additional 24 h (MPs/Platelets/A549 = 5000/250/1). The samples with or without Trypan blue quenching allow us to differentiate and quantify the fluorescent particles that have been completely engulfed versus those that are merely adhering to the cell membrane. Trypan blue quenches the fluorescence of the HAS-MPs left on the surface of the cells. The flow cytometer quantified the cellular uptake percentage and MFI of A549 cells.

### 3.10. Validation of CD62P Ligand Expression Level in TCGA and CCLE Databases

CD62P binds to several common ligands, including CD44, SELPLG, and CD24. The Cancer Cell Line Encyclopedia (CCLE) project (accessed on 6 July 2022, <https://www.broadinstitute.org/ccle>) was used to validate the expression profiles of CD44 and SELPLG in 1091 cell lines. The Cancer Genome Atlas (TCGA) database (accessed on 7 July 2022, <https://portal.gdc.cancer.gov/>) was used to validate the CD44 and SELPLG expression in 33 cancers. Different gene expression analysis was performed using the limma package in R studio software to determine whether CD44 or SELPLG expression varied between tumors and normal tissues.

### 3.11. Statistical Analysis

In addition to the statistical methods mentioned above, Student's *t*-test was used to explore the association between the groups. Data were expressed as mean  $\pm$  standard deviations (SD). \*  $p < 0.05$ , \*\*  $p < 0.01$ , and \*\*\*  $p < 0.001$  were thought to be statistically significant.

## 4. Conclusions

In this study, anti-CD41-HSA-MPs were designed to target CTCs by hitchhiking on platelets to track tumor cells. CD62P-HSA-MPs were used to adhere the tumor cells by taking advantage of the conjugation of CD62P. Both resultant modified HSA-MPs demonstrated the tumor cell-targeting ability in vitro. In summary, the platelet-based and platelet-mimicking human serum albumin submicron particles offered a promising approach for metastatic cancer therapy and tracking through accurate targeting for tumor cells.

**Author Contributions:** Conceptualization, H.B. and R.G.; methodology, H.B.; software, X.Z. and P.R.; validation, H.B. and R.G.; formal analysis, X.Z.; investigation, X.Z., P.R., M.H., L.-E.H.O. and M.M.-d.A.; resources, H.B.; data curation, H.B.; writing—original draft preparation, X.Z.; writing—review and editing, H.B. and R.G.; visualization, X.Z.; supervision, H.B.; project administration, H.B.; funding acquisition, H.B. All authors have read and agreed to the published version of the manuscript.

**Funding:** This research was funded by the Chinese Scholarship Council, grant number (CSC NO.201908320284) and by H2020 MSCA-Rise 2018 project OXIGENATED, grant number 823879.

**Institutional Review Board Statement:** The study was conducted in accordance with the Declaration of Helsinki and approved by the Ethics Committee of Charité (EA1/110/21).

**Informed Consent Statement:** Informed consent was obtained from all subjects involved in the study.

**Data Availability Statement:** The data that support the findings of this study are available from the corresponding author upon reasonable request. The datasets generated and analyzed during the current study are available in the TCGA database (<https://portal.gdc.cancer.gov/>) and the CCLE database (<https://www.broadinstitute.org/ccle>).

**Acknowledgments:** We would also like to thank Wanit Chaisorn for technical support on this study. X.Z. thanks Wen Liu for the support of his research.

**Conflicts of Interest:** The authors declare no conflict of interest.

## References

- Chang, Y.S.; di Tomaso, E.; McDonald, D.M.; Jones, R.; Jain, R.K.; Munn, L.L. Mosaic blood vessels in tumors: Frequency of cancer cells in contact with flowing blood. *Proc. Natl. Acad. Sci. USA* **2000**, *97*, 14608–14613. [[CrossRef](#)]
- Caramel, J.; Papadogeorgakis, E.; Hill, L.; Browne, G.J.; Richard, G.; Wierinckx, A.; Saldanha, G.; Osborne, J.; Hutchinson, P.; Tse, G.; et al. A Switch in the Expression of Embryonic EMT-Inducers Drives the Development of Malignant Melanoma. *Cancer Cell* **2013**, *24*, 466–480. [[CrossRef](#)]
- Hanahan, D.; Weinberg, R.A. Hallmarks of cancer: The next generation. *Cell* **2011**, *144*, 646–674. [[CrossRef](#)]
- Dongre, A.; Weinberg, R.A. New insights into the mechanisms of epithelial-mesenchymal transition and implications for cancer. *Nat. Rev. Mol. Cell Biol.* **2018**, *20*, 69–84. [[CrossRef](#)]
- Peralta, M.; Osmani, N.; Goetz, J.G. Circulating tumor cells: Towards mechanical phenotyping of metastasis. *iScience* **2022**, *25*, 103969. [[CrossRef](#)]
- Follain, G.; Osmani, N.; Azevedo, A.S.; Allio, G.; Mercier, L.; Karreman, M.A.; Solecki, G.; Leòn, M.J.G.; Lefebvre, O.; Fekonja, N.; et al. Hemodynamic Forces Tune the Arrest, Adhesion, and Extravasation of Circulating Tumor Cells. *Dev. Cell* **2018**, *45*, 33–52.e12. [[CrossRef](#)]
- Gay, L.J.; Felding-Habermann, B. Contribution of platelets to tumour metastasis. *Nat. Cancer* **2011**, *11*, 123–134. [[CrossRef](#)]
- Li, N. Platelets in cancer metastasis: To help the “villain” to do evil. *Int. J. Cancer* **2016**, *138*, 2078–2087. [[CrossRef](#)]
- Placke, T.; Örgel, M.; Schaller, M.; Jung, G.; Rammensee, H.-G.; Kopp, H.-G.; Salih, H.R. Platelet-Derived MHC Class I Confers a Pseudonormal Phenotype to Cancer Cells That Subverts the Antitumor Reactivity of Natural Killer Immune Cells. *Cancer Res.* **2012**, *72*, 440–448. [[CrossRef](#)]
- Schumacher, D.; Strilic, B.; Sivaraj, K.K.; Wettschureck, N.; Offermanns, S. Platelet-derived nucleotides promote tumor-cell transendothelial migration and metastasis via P2Y2 receptor. *Cancer Cell* **2013**, *24*, 130–137. [[CrossRef](#)]
- Schlesinger, M. Role of platelets and platelet receptors in cancer metastasis. *J. Hematol. Oncol.* **2018**, *11*, 125. [[CrossRef](#)]
- Lucotti, S.; Muschel, R.J. Platelets and Metastasis: New Implications of an Old Interplay. *Front. Oncol.* **2020**, *10*, 1350. [[CrossRef](#)]
- Han, X.; Chen, J.; Chu, J.; Liang, C.; Ma, Q.; Fan, Q.; Liu, Z.; Wang, C. Platelets as platforms for inhibition of tumor recurrence post-physical therapy by delivery of anti-PD-L1 checkpoint antibody. *J. Control. Release* **2019**, *304*, 233–241. [[CrossRef](#)]
- Hu, Q.; Sun, W.; Wang, J.; Ruan, H.; Zhang, X.; Ye, Y.; Shen, S.; Wang, C.; Lu, W.; Cheng, K.; et al. Conjugation of haematopoietic stem cells and platelets decorated with anti-PD-1 antibodies augments anti-leukaemia efficacy. *Nat. Biomed. Eng.* **2018**, *2*, 831–840. [[CrossRef](#)]
- Hu, Q.; Sun, W.; Qian, C.; Wang, C.; Bomba, H.N.; Gu, Z. Anticancer Platelet-Mimicking Nanovehicles. *Adv. Mater.* **2015**, *27*, 7043–7050. [[CrossRef](#)]
- Li, J.; Ai, Y.; Wang, L.; Bu, P.; Sharkey, C.C.; Wu, Q.; Wun, B.; Roy, S.; Shen, X.; King, M.R. Targeted drug delivery to circulating tumor cells via platelet membrane-functionalized particles. *Biomaterials* **2016**, *76*, 52–65. [[CrossRef](#)]
- Ay, C.; Simanek, R.; Vormittag, R.; Dunkler, D.; Alguel, G.; Koder, S.; Kornek, G.; Marosi, C.; Wagner, O.; Zielinski, C.; et al. High plasma levels of soluble P-selectin are predictive of venous thromboembolism in cancer patients: Results from the Vienna Cancer and Thrombosis Study (CATS). *Blood* **2008**, *112*, 2703–2708. [[CrossRef](#)]
- Larsen, M.T.; Kuhlmann, M.; Hvam, M.L.; Howard, K.A. Albumin-based drug delivery: Harnessing nature to cure disease. *Mol. Cell. Ther.* **2016**, *4*, 3. [[CrossRef](#)]



19. Koziol, M.J.; Sievers, T.K.; Smuda, K.; Xiong, Y.; Müller, A.; Wojcik, F.; Steffen, A.; Dathe, M.; Georgieva, R.; Bäuml, H. Kinetics and Efficiency of a Methyl-Carboxylated 5-Fluorouracil-Bovine Serum Albumin Adduct for Targeted Delivery. *Macromol. Biosci.* **2013**, *14*, 428–439. [[CrossRef](#)]
20. Bolling, C.; Graefe, T.; Lübbling, C.; Jankevicius, F.; Uktveris, S.; Cesas, A.; Meyer-Moldenhauer, W.-H.; Starkmann, H.; Weigel, M.; Burk, K.; et al. Phase II study of MTX-HSA in combination with Cisplatin as first line treatment in patients with advanced or metastatic transitional cell carcinoma. *Investig. New Drugs* **2006**, *24*, 521–527. [[CrossRef](#)]
21. Vis, A.N.; van der Gaast, A.; van Rhijn, B.W.; Catsburg, T.K.; Schmidt, C.; Mickisch, G.H. A phase II trial of methotrexate-human serum albumin (MTX-HSA) in patients with metastatic renal cell carcinoma who progressed under immunotherapy. *Cancer Chemother. Pharmacol.* **2002**, *49*, 342–345. [[PubMed](#)]
22. Fabi, A.; Giannarelli, D.; Malaguti, P.; Ferretti, G.; Vari, S.; Papaldo, P.; Nisticò, C.; Caterino, M.; De Vita, R.; Mottolese, M.; et al. Prospective study on nanoparticle albumin-bound paclitaxel in advanced breast cancer: Clinical results and biological observations in taxane-pretreated patients. *Drug Des. Dev. Ther.* **2015**, *9*, 6177–6183. [[CrossRef](#)] [[PubMed](#)]
23. Murphy, C.; Muscat, A.; Ashley, D.; Mukaro, V.; West, L.; Liao, Y.; Chisanga, D.; Shi, W.; Collins, I.; Baron-Hay, S.; et al. Tailored NEOadjuvant epirubicin, cyclophosphamide and Nanoparticle Albumin-Bound paclitaxel for breast cancer: The phase II NEONAB trial—Clinical outcomes and molecular determinants of response. *PLoS ONE* **2019**, *14*, e0210891. [[CrossRef](#)] [[PubMed](#)]
24. Bäuml, H.; Georgieva, R. Coupled Enzyme Reactions in Multicompartment Microparticles. *Biomacromolecules* **2010**, *11*, 1480–1487. [[CrossRef](#)] [[PubMed](#)]
25. Xiong, Y.; Liu, Z.Z.; Georgieva, R.; Smuda, K.; Steffen, A.; Sendeski, M.; Voigt, A.; Patzak, A.; Bäuml, H. Nonvasoconstrictive Hemoglobin Particles as Oxygen Carriers. *ACS Nano* **2013**, *7*, 7454–7461. [[CrossRef](#)]
26. Xiong, Y.; Steffen, A.; Andreas, K.; Müller, S.; Sternberg, N.; Georgieva, R.; Bäuml, H. Hemoglobin-Based Oxygen Carrier Microparticles: Synthesis, Properties, and In Vitro and In Vivo Investigations. *Biomacromolecules* **2012**, *13*, 3292–3300. [[CrossRef](#)]
27. Chaiwaree, S.; Prapan, A.; Suwannasom, N.; Laporte, T.; Neumann, T.; Pruß, A.; Georgieva, R.; Bäuml, H. Doxorubicin-Loaded Human Serum Albumin Submicron Particles: Preparation, Characterization and In Vitro Cellular Uptake. *Pharmaceutics* **2020**, *12*, 224. [[CrossRef](#)]
28. Suwannasom, N.; Smuda, K.; Kloypan, C.; Kaewprayoon, W.; Baisaeng, N.; Prapan, A.; Chaiwaree, S.; Georgieva, R.; Bäuml, H. Albumin Submicron Particles with Entrapped Riboflavin—Fabrication and Characterization. *Nanomaterials* **2019**, *9*, 482. [[CrossRef](#)]
29. Kim, Y.J.; Borsig, L.; Han, H.-L.; Varki, N.M.; Varki, A. Distinct Selectin Ligands on Colon Carcinoma Mucins Can Mediate Pathological Interactions among Platelets, Leukocytes, and Endothelium. *Am. J. Pathol.* **1999**, *155*, 461–472. [[CrossRef](#)]
30. Chen, M.; Geng, J.-G. P-selectin mediates adhesion of leukocytes, platelets, and cancer cells in inflammation, thrombosis, and cancer growth and metastasis. *Arch. Immunol. Ther. Exp.* **2006**, *54*, 75–84. [[CrossRef](#)]
31. Nolo, R.; Herbrich, S.; Rao, A.; Zweidler-McKay, P.; Kannan, S.; Gopalakrishnan, V. Targeting P-selectin blocks neuroblastoma growth. *Oncotarget* **2017**, *8*, 86657–86670. [[CrossRef](#)] [[PubMed](#)]
32. Bäuml, H.; Xiong, Y.; Liu, Z.Z.; Patzak, A.; Georgieva, R. Novel Hemoglobin Particles—Promising New-Generation Hemoglobin-Based Oxygen Carriers. *Artif. Organs* **2014**, *38*, 708–714. [[CrossRef](#)] [[PubMed](#)]
33. Yumoto, R.; Suzuka, S.; Oda, K.; Nagai, J.; Takano, M. Endocytic Uptake of FITC-albumin by Human Alveolar Epithelial Cell Line A549. *Drug Metab. Pharmacokinet.* **2012**, *27*, 336–343. [[CrossRef](#)] [[PubMed](#)]
34. A Joosse, S.; Gorges, T.M.; Pantel, K. Biology, detection, and clinical implications of circulating tumor cells. *EMBO Mol. Med.* **2014**, *7*, 1–11. [[CrossRef](#)]
35. Meng, S.; Tripathy, D.; Frenkel, E.P.; Shete, S.; Naftalis, E.Z.; Huth, J.F.; Beitsch, P.D.; Leitch, M.; Hoover, S.; Euhus, D.; et al. Circulating Tumor Cells in Patients with Breast Cancer Dormancy. *Clin. Cancer Res.* **2004**, *10*, 8152–8162. [[CrossRef](#)]
36. Rahman, S.M.; Hlady, V. Downstream platelet adhesion and activation under highly elevated upstream shear forces. *Acta Biomater.* **2019**, *91*, 135–143. [[CrossRef](#)]
37. Desai, N.; Trieu, V.; Damascelli, B.; Soon-Shiong, P. SPARC Expression Correlates with Tumor Response to Albumin-Bound Paclitaxel in Head and Neck Cancer Patients. *Transl. Oncol.* **2009**, *2*, 59–64. [[CrossRef](#)]
38. Merlot, A.M.; Kalinowski, D.S.; Richardson, D.R. Unraveling the mysteries of serum albumin—more than just a serum protein. *Front. Physiol.* **2014**, *5*, 299. [[CrossRef](#)]
39. Schnitzer, J.E.; Oh, P. Albondin-mediated capillary permeability to albumin. Differential role of receptors in endothelial transcytosis and endocytosis of native and modified albumins. *J. Biol. Chem.* **1994**, *269*, 6072–6082. [[CrossRef](#)]
40. Chen, J.-L.; Peng, S.-W.; Ko, W.-H.; Yeh, M.-K.; Chiang, C.-H. The mechanism of high transfection efficiency of human serum albumin conjugated polyethylenimine in A549 cells. *J. Med. Sci.* **2015**, *35*, 57–61. [[CrossRef](#)]
41. Felding-Habermann, B.; Habermann, R.; Saldivar, E.; Ruggeri, Z.M. Role of beta3 integrins in melanoma cell adhesion to activated platelets under flow. *J. Biol. Chem.* **1996**, *271*, 5892–5900. [[CrossRef](#)] [[PubMed](#)]
42. Suzuki-Inoue, K.; Kato, Y.; Inoue, O.; Kaneko, M.K.; Mishima, K.; Yatomi, Y.; Yamazaki, Y.; Narimatsu, H.; Ozaki, Y. Involvement of the Snake Toxin Receptor CLEC-2, in Podoplanin-mediated Platelet Activation, by Cancer Cells. *J. Biol. Chem.* **2007**, *282*, 25993–26001. [[CrossRef](#)] [[PubMed](#)]
43. Yu, L.-X.; Yan, L.; Yang, W.; Wu, F.-Q.; Ling, Y.; Chen, S.Z.; Tang, L.; Tan, Y.-X.; Cao, D.; Wu, M.-C.; et al. Platelets promote tumour metastasis via interaction between TLR4 and tumour cell-released high-mobility group box1 protein. *Nat. Commun.* **2014**, *5*, 5256. [[CrossRef](#)] [[PubMed](#)]

44. Gong, L.; Cai, Y.; Zhou, X.; Yang, H. Activated Platelets Interact with Lung Cancer Cells through P-Selectin Glycoprotein Ligand-1. *Pathol. Oncol. Res.* **2012**, *18*, 989–996. [[CrossRef](#)] [[PubMed](#)]
45. Aigner, S.; Ramos, C.L.; Hafezi-Moghadam, A.; Lawrence, M.B.; Friederichs, J.; Altevogt, P.; Ley, K. CD24 mediates rolling of breast carcinoma cells on P-selectin. *FASEB J.* **1998**, *12*, 1241–1251. [[CrossRef](#)]
46. Dimitroff, C.J.; Descheny, L.; Trujillo, N.; Kim, R.; Nguyen, V.; Huang, W.; Pienta, K.J.; Kutok, J.L.; Rubin, M.A. Identification of Leukocyte E-Selectin Ligands, P-Selectin Glycoprotein Ligand-1 and E-Selectin Ligand-1, on Human Metastatic Prostate Tumor Cells. *Cancer Res.* **2005**, *65*, 5750–5760. [[CrossRef](#)]
47. Vega, F.M.; Colmenero-Repiso, A.; Gómez-Muñoz, M.A.; Rodríguez-Prieto, I.; Aguilar-Morante, D.; Ramírez, G.; Márquez, C.; Cabello, R.; Pardal, R. CD44-high neural crest stem-like cells are associated with tumour aggressiveness and poor survival in neuroblastoma tumours. *eBioMedicine* **2019**, *49*, 82–95. [[CrossRef](#)]
48. Wang, C.Y.; Huang, C.S.; Yang, Y.P.; Liu, C.Y.; Liu, Y.Y.; Wu, W.W.; Lu, K.H.; Chen, K.H.; Chang, Y.L.; Lee, S.D.; et al. The subpopulation of CD44-positive cells promoted tumorigenicity and metastatic ability in lung adenocarcinoma. *J. Chin. Med. Assoc.* **2019**, *82*, 196–201. [[CrossRef](#)]
49. Xu, H.; Niu, M.; Yuan, X.; Wu, K.; Liu, A. CD44 as a tumor biomarker and therapeutic target. *Exp. Hematol. Oncol.* **2020**, *9*, 36. [[CrossRef](#)]
50. Zanjani, L.S.; Madjd, Z.; Abolhasani, M.; Rasti, A.; Fodstad, O.; Andersson, Y.; Asgari, M. Increased expression of CD44 is associated with more aggressive behavior in clear cell renal cell carcinoma. *Biomark. Med.* **2018**, *12*, 45–61. [[CrossRef](#)]
51. Holme, P.A.; Ørvim, U.; Hamers, M.J.A.G.; Solum, N.O.; Brosstad, F.R.; Barstad, R.M.; Sakariassen, K.S. Shear-Induced Platelet Activation and Platelet Microparticle Formation at Blood Flow Conditions as in Arteries With a Severe Stenosis. *Arter. Thromb. Vasc. Biol.* **1997**, *17*, 646–653. [[CrossRef](#)] [[PubMed](#)]



## **Curriculum Vitae**

My curriculum vitae does not appear in the electronic version of my paper for reasons of data protection.

## Publication list

1. **Zhao, X.**; Georgieva, R.; Rerkshanandana, P.; Hackmann, M.; Heil Olaizola, L.-E.; Müller-de Ahna, M.; Bäuml, H. Tumor Cell Capture Using Platelet-Based and Platelet-Mimicking Modified Human Serum Albumin Submicron Particles. *Int. J. Mol. Sci.* 2022, *23*, 14277. <https://doi.org/10.3390/ijms232214277>. (IF=6.208)
2. **Zhao XT**, Zhu Y, Zhou JF, Gao YJ, Liu FZ. Development of a novel 7 immune-related genes prognostic model for oral cancer: A study based on TCGA database. *Oral Oncol.* 2021;*112*:105088. doi:10.1016/j.oraloncology.2020.105088. (IF=5.972)
3. Liu F, **Zhao X**, Qian Y, Zhang J, Zhang Y, Yin R. MiR-206 inhibits Head and neck squamous cell carcinoma cell progression by targeting HDAC6 via PTEN/AKT/mTOR pathway. *Biomed Pharmacother.* 2017;*96*:229-237. doi:10.1016/j.biopha.2017.08.145. (IF=7.419)
4. **Zhao X**, Liu F, Zhang Y, Li P. Prognostic and clinicopathological significance of Gankyrin overexpression in cancers: evidence from a meta-analysis. *Onco Targets Ther.* 2016;*9*:1961-1968. Published 2016 Apr 4. doi:10.2147/OTT.S101687. (IF=4.345)

## Acknowledgments

I would like to express my deepest appreciation to my first supervisor Prof. Dr. Hans Bäumlner. I believe he is a great epitome of enthusiasm, perseverance and dedication to science. I sincerely appreciate his supervision of my scientific research practice through my wonderful and unforgettable time in Charité, for his sincere encouragement, dedicated support, and constructive advice. The kind of knowledge, affection and cognizance showered upon me has left a long-lasting impression on my scientific soul. He is always kind, patient that has made my stay in Berlin worthwhile

I would also like to express my heartfelt acknowledgment to my supervisor Dr. Radosztina Georgieva for her critical assessment, affectionate words and ever available patience always. Her motivation kept me charged and motivated to give my best shot even in a letdown situation. I am beyond the reachability of words to express my thankfulness for her support and guidance.

Many thanks to my colleagues and friends in our laboratory, Chaisorn, Wanit, Dr. Yu Xiong, Pichayut Rerkshanandana, Moritz Hackmann, Lara-Elena Heil Olaizola, Maxine Müller-de Ahna for their strong support in my project and life care in Berlin.

I would like to thank all my friends Yao Chen, Yu Zhang and all others for always being with me and supporting me throughout a well.

Words are not sufficient to express my regards to Mama, Papa, and my wife for their patience, care, affection, support and understanding; they are thanked for the sacrifices they cheerfully underwent.